EOM-3901
Master's Thesis in
Energy, Climate and Environment

Estimating Production Loss due to Icing on Wind Turbines

Silje Sanderud Haaland

June, 2011

FACULTY OF SCIENCE AND TECHNOLOGY
Department of Physics and Technology
University of Tromsø

EOM-3901
Master's Thesis in
Energy, Climate and Environment

Estimating Production Loss due to Icing on Wind Turbines

Silje Sanderud Haaland

June, 2011

FACULTY OF SCIENCE AND TECHNOLOGY
Department of Physics and Technology
University of Tromsø

Acknowledgment

Lett skjelven og med langt over hvilepuls er jeg i ferd med å sette strek for noe som til tider har kjentes ut som et evigvarende prosjekt.

Det er antagelig ikke det smarteste å velge å skrive master i et emne som verken en selv eller noen på ens eget universitet egentlig vet særlig mye om...Men så fantastisk det er å få det til! Yngve, min veileder, som antagelig har lært like mye som meg om vindturbiner og is i løpet av 5 måneder, tusen takk. Din iver etter kunnskap, og dine oppmuntringer har vært uvurderlige. Stor takk til Veileder Knut på Kjeller, som har vært den som vet alt, har stor erfaring i emnet og også har rettet oppgaven steg for steg. Øyvind, matlabguden, fortjener også en stor takk.

En stor takk til alle på norutbrakka som stort sett alltid har hatt et svar på mine programmerings problemer, og ikke minst vært godt selskap. Kompileringseksperten Thomas spesielt. Kristine, takk for at du til tider har vært like lei, glad, positiv og desperat nedbrutt som meg og likevel villet snakke med meg. Takk også for at du har klagd, i baljer og svømmebasseng, og dermed latt meg få lov til å gjøre det samme. Du er en unik samarbeidspartner! Takk Eldar, for at du har holdt ut med mine opp og nedturer i 5 måneder og i tillegg har hatt klokketro på at jeg skulle klare dette.

Abstract

Icing on wind turbines are known to lower their performance, but the exact relationship between wind, ice and power production is not known. In this thesis power loss due to icing on turbine blades at Aapua wind park is investigated for the winter season 2009-2010. The total loss is found to be 30%, whereof 25% is concluded being due to icing.

Three different methods are presented to estimate a power output model $\hat{P}(V, I)$, based on empirical data of wind speed, ice load and power production from a wind turbine. The models estimate power output from wind speed and ice load observations. Their performance are compared using correlation and root mean square error (RMSE), and the kriging method, using a weighted mean to calculate power output, is found best.

A comparison of the proposed kriging model to an existing model show a 10% increase in performance for the kriging method. Testing shows that kriging works well for low wind speeds and low ice loads, but tends to overestimate production during high ice loads. For the season as a whole, the modelled power output underestimates the power production with 1%. The best result is found in March with 1% deviation from the measured output, and the worst in January, with an overproduction of 24%.

Time series of modelled, measured and expected power output, together with ice load and temperature measurements, are investigated. Results show that sublimation, shedding, melting and accretion processes on the turbine wings, are not fully captured by the model.

Mismatch between ice loads on measuring equipment compared to turbine blades, together with insufficient number of observation data, are found to be the main reasons for inaccuracy in the model. More observation data, especially for high wind speed and ice load classes, in addition to improved quality of ice load measurements, could improve the model significantly.

Contents

Chapter 1

Introduction

Atmospheric icing is a problem related to cold regions. Arctic and sub arctic areas are intuitively exposed to atmospheric icing, as is high altitude areas. Also, further south in lower laying regions, atmospheric icing in the form of super-cooled rain may be a significant problem.

In Norway and Sweden, atmospheric icing on structures is most frequently due to in-cloud icing. This happens when the temperature is below 0^oC and the cloud base is sufficiently low to cover the constructions. Clouds below freezing temperature may contain large amounts of water droplets which has not yet frozen to ice crystals. When these droplets hit an unheated construction they freeze spontaneously covering it with a layer of ice. The characteristics of the ice, density, colour etc is depending on the meteorological conditions at the time. Structures like turbine blades, power lines, measuring equipment and towers may suffer severe damage due to icing. In 1961 there was observed an extreme icing event at Lønahorgi in Voss, Norway [Fikke, 1980]. 305 kg of ice per meter was measured on a power cable. This is the biggest ice load recorded world wide and it did cause severe damage. Heavy icing may cause damage by simply making the construction collapse as the load gets too big. Malfunction of instruments or smaller breakdowns due to icing are more common. For instance, unheated cup anemometers and wind vanes do not function during icing conditions, and may be out of function until the ice has disappeared.

Wind turbines are usually put up in areas exposed to extreme weather conditions. Typically on top of mountains where wind speeds in general are higher. This also makes the turbine exposed to clouds and atmospheric icing. As ice is accreting the turbine and surroundings is affected in several ways:

- Ice loads on the blades may lead to vibrations, resonance and cause unbal-

ance between blades. All this may lead to mechanical failure and fatigue fracture.

- Ice shedding may cause a risk for both maintenance workers and people living or hiking in an area close to wind turbines. Calculation of the probability for people being hit by ice throws from turbines has been done [Battisti et al., 2005].
- The aerodynamics of turbine wings are optimally designed to utilize the airflow to produce power. A layer of ice on the turbine blades will alter their aerodynamic form and lower the turbine's production [Parent and Ilinca, 2011].

The ability to predict icing events and their severity at a specific location is, for the given reasons, important. Especially when planning and building new wind farms, the cost effectiveness is of high interest to investors. Icing conditions will influence both the power output from a wind park and maintenance cost.

For operating wind farms, estimating the production loss more accurately and time dissolved intervals is of high interest. An estimate of the production for the next day is needed as the farm owners must inform how much electricity they can deliver the next day.

1.1 Former research

Wind energy as a power industry has developed a lot during the last years. Wind energy is used all over the world and also the amount of wind farms in cold regions is increasing. Wind power in cold climate has been given more and more attention through the International Energy Agency's (IEA) emphasis on cold climate regions [Laakso et al., 2009]. IEA has specified that one of its objectives is to find methods to better estimate the effect of ice accretion on energy production. EU is also addressing wind energy in cold climate as an important topic. The COST727 project, started in April 2004, is an EU cooperation including 3 different research groups working on physics, modeling, measuring and forecasting related to icing. The conference International Workshop on Atmospheric Icing (IWAIS), which is held every second or third year, is also a useful contributor to the international work on cold climate wind energy. Presented work and review of part of the COST727 action can be found in the proceedings of IWAIS from 2007 and 2009 at www.seppyo.org and www.IWAIS2009.ch.

Makkonen presented in 2000 what is now used as the ground principals for modeling of ice growth [Makkonen, 2000]. Theory on the physics and processes controlling ice accumulation are discussed. A formula for ice growth based on wind

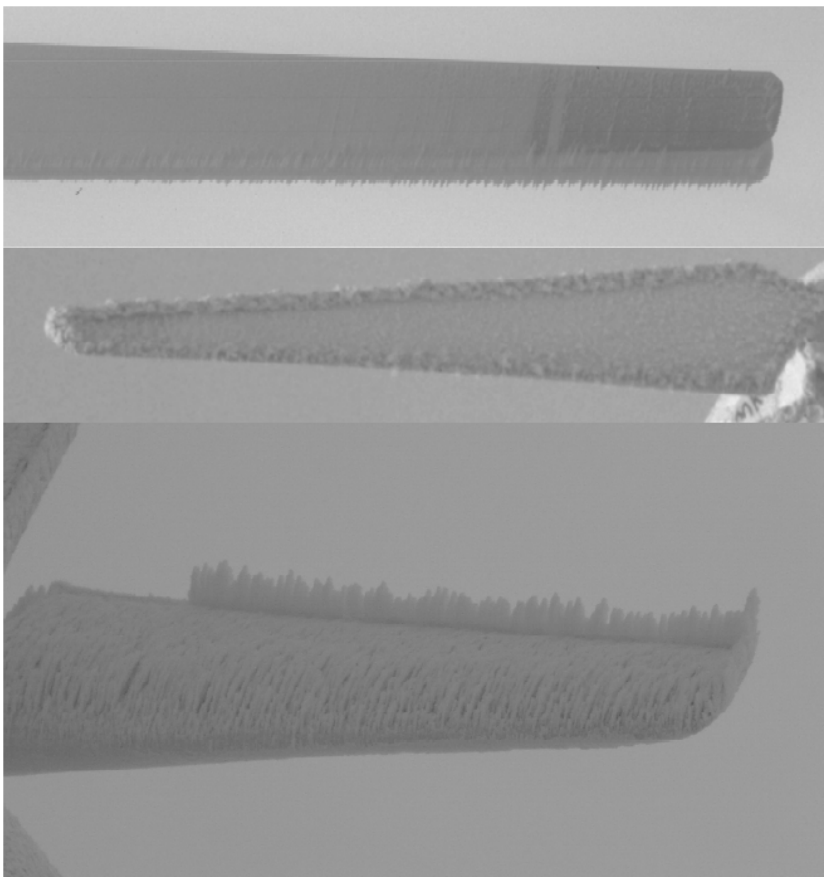

Figure 1.1: Typical ice accretion at leading edge of a rotor blade. Top picture shows an operating rotor, middle a rotor in low winds and at the bottom the blade is standing still. Figure from [Tammelin and Seifert, 2001]

speed and water content is presented, and uncertainties concerning the calculations are pointed out. It is shown how icing rate on an object varies according to wind speed, temperature, precipitation, liquid water content (LWC), cloud water droplet size and size of the object. Those parameters also define the size of three efficiency parameters; Collision, sticking and accretion efficiency. Today this theory is the basis for all accumulation models for icing and much of the theory is used in the international standard for icing on structures [ISO12494, 2001].

The theory from [Makkonen, 2000] is used many places, e.g. to develop the TURBICE model [Makkonen et al., 2001]. This is a numerical model which simulates the amount and shape of ice accreted on wind turbine blades. The model includes both in-cloud rime icing and glaze icing due to precipitation.

[Drage, 2005] carried out ice measurements on two sites in Norway. A cylindrical stick rotating freely accreted ice and its weight was measured. His measurements are useful when comparing modeled and measured ice. Drage compared the measurements to modeled ice loads and found, as in several other investigations that modeled ice using meso-scale numerical models, is underestimated.

The ability of numerical weather prediction models to simulate icing has improved the last years. Weather research and forecasting model (WRF), is a meso-scale widely used model for this propose. Information about the modeling system can be found at their homepage http://wrf-model.org and also in [Michalakes et al., 2001]. An improvement to the microphysics scheme used in the WRF-model was done by [Thompson et al., 2008]. The improvement plays a major role in the simulation of super cooled liquid water. Water content is critical to ice growth and is one of the parameters needed in in-cloud icing accretion models. A new cloud and precipitation physics scheme is newly developed and is described in [Thompson et al., 2009]. This was a major contribution to simulate the median volume diameter (MVD) of the supercooled water droplets to use in accretion models.

In 2009, Ø. Byrkjedal and E. Berge [Øyvind Byrkjedal and Berge, 2009] used the meso-scale weather model, WRF, to develop a regional wind resource map over Norway, and the results were used further to develop icing maps for the same region. The WRF-model produce vertical profiles of wind, temperature and cloud water content. The results were then used as input to an ice accretion model to calculate in-cloud icing on a reference object. The weather forecast model is in this way used to also predict icing.

In [Nygaard, 2009] a numerical weather prediction model (NWP), in combination with a cylindrical rime ice accretion model, was applied to simulate icing events on six different test stations. Ice load measurements were carried out on the test stations with an Ice Monitor during the whole winter season 2007/2008. Most

icing events occurred during strong temperature inversions which are not predicted very well by NWP models. This leads to incorrect prediction of ice, mostly due to the sensitivity of the simulation of LWC. However, one test site experienced icing in relation to a frontal system. Here the NWP preformed relatively well. In general, an underestimation of ice due to terrain blending, were height of the terrain in the model differs from the real height, was found. Also the importance of a correct volume number concentration was found; The MVD is closely related to the number concentration of droplets (N_c) which is also critical when simulating ice. Nygaard (2009) shows that an increase in N_c from 100 cm^{-3} to 300 cm^{-3}, reduces the simulated ice load by approximately 40%. Case studies with very high horisontal resolution is suggested to remove the effect of terrain blending.

Some early attempts to model ice accretion using observation data has been done for example by [Sundin and Makkonen, 1997] where data from a weather station was used to model ice loads on a 300 m tower 3 km from the weather station. Assumptions on the vertical profile were done to extrapolate the weather data to the wanted height, and a simple icing model was used to calculate the ice load. The results were quite good for longer periods, a whole winter, but tend to fail when ice melted and fell off the tower during warmer periods.

Another method was presented by [Harstveit, 2002]. The use of meteorological data was combined with Metar data from an airport to calculate in-cloud icing on a reference object. Metar-data provided cloud observations which was used to estimate the liquid water content of air. The observations and results of estimated cloud water content were then used in the ice accretion formula to estimate icing on a reference object. In addition an energy balance equation modified the accretion model to allow for ice shedding. In [Harstveit, 2009] the method was validated by applying the model on different sites in Norway where icing measurements exist. The modeled ice was compared to three observations sites showing a nice coincidence between observed and modeled ice when the shedding factor was tuned.

In [Harstveit et al., 2009] a validation of the use of WRF-simulations to produce in-cloud icing maps was performed. The results from WRF-simulations were compared to results produced using the method from [Harstveit, 2002]. An excellent coincidence between the statistics of the results was found above 500masl.

The mentioned models for ice accumulation are for ice growth on structures. In 1998 [Seifert and Richert, 1998] presented a model to estimate the consequences of ice on rotor blades. Different ice shapes where collected and cataloged. The shapes where then reconstructed and mounted on the edge of turbine blades. The blades, both clean and with different ice shapes, where tested in a wind tunnel. The altered aerodynamics and loads where registered, the effect of the ice was

calculated and loss in performance due to the ice shapes estimated. A recipe to estimate loads and aerodynamics of turbine blades where then presented.

Research on atmospheric icing and the effect of ice shapes on turbine blades has increased during the last ten years. In [Øyvind Byrkjedal, 2009], results from the wind resource map and icing map for the same region was used to estimate production loss for wind turbines due to the modeled icing conditions. Expected production for a chosen turbine was calculated by combining power curve and simulated wind speed from the wind resource map. The icing map was then used to estimate production loss due to in-cloud icing in the same area. Results showed an average loss of between 14% and 22%, depending on the method used to estimate icing periods.

[Homola et al., 2009] estimated the production loss due to iced blades and meteorological instruments for three different wind power sites in Norway and Sweden in 2009. They used the measured wind speed to estimate the expected power output and compared it to the measured output. Ice loads where measured at certain times and an estimate on how much power loss was due to icing was calculated. At the most severe icing site a loss of 28% was found during wintertime. The numbers are thought to be underestimated, mainly because of the calculation method. The uncertainty, however, is large [Homola et al., 2009]. A lot of research on ice sensors has also been performed [Homola et al., 2006].

To calculate the annual power output for a wind turbine at a specific location, both the site wind profile and icing conditions need to be taken into account [Tammelin and Seifert, 2001]. The influence of icing events on turbines performance has been investigated and annual losses between 17% to 30% have been found on ice exposed sites [Barber et al., 2009, Øyvind Byrkjedal, 2009, Homola et al., 2009]. Still there is not sufficient knowledge about icing to accurately predict production losses, especially in shorter time resolution.

It has been, and still is, a major challenge to validate ice predicting models. No routine measurements of icing exist today. Only measuring of meteorological data like wind speed, temperature, air humidity etc. are run on a regular basis. Validation of the modeled ice has been performed using other methods, as explained. Still it is a big challenge to come up with reliable ice measurements that can validate models [Pers comm. S. Fikke].

1.2 Purpose of the study

The aim of this thesis is to find a more accurate connection between icing events and the loss in production at wind farms exposed to icing. This will hopefully lead

to a better understanding of how ice affect the turbines performance, and help develop models to estimate production in cold climate more accurately. A model for estimating power output for a given wind speed and ice load is developed and compared to an existing model made by Øyvind Byrkjedal after an idea from [Seifert and Richert, 1998].

The interrelationship between ice load measurements at a wind turbine site, Aapua wind park, and the observed power produced during the winter season 2009-2010 will be analyzed. One big challenge is to be able to give improved production estimates with high time resolution. Until now, research on production loss due to icing is estimated quite accurately considering a whole year. Shorter periods are highly inaccurate and needs to be better estimated.

Meteorological equipment measuring wind speed, temperature, air humidity, air density and air pressure is stationed at each turbine. Ice load is measured at one site close to one of the turbines and production data is given from the O2 company owning the wind farm. Estimating production loss due to icing is a difficult task. A number of parameters are influencing the actual output from a turbine, and ice is one of the factors that can reduce the output.

As wind power is developing and more of the power market is provided by wind energy, the wind will influence electricity prices. Icing conditions can develop an influence if the cold region turbines are delivering a significant amount of electricity to the grid. Being able to predict production in cold climate and ice exposed areas will then be of high importance. Short term estimates of production are needed for farm owners to predict the next days production. A more accurate loss due to icing could improve these estimates.

The assignment is given by Kjeller Vindteknikk by Dr. Knut Harstveit. He has been working on icing conditions in many areas. Øyvind Byrkjedal, from Kjeller Vindteknikk is also working with icing and has played a role in forming the assignment.

1.3 Structure of report

The report is structured as follows. Chapter 2 includes relevant theory on wind turbines, how they extract and produce energy, and then aerodynamic lift is explained. Theory on the occurrence of atmospheric icing including meteorology is also presented. Chapter 3 gives information of how data is collected and presents the methods used for cleaning of the data. Calculations of production and production loss and also statistical methods used in model making are explained. Chapter 4 presents results from calculations and results from testing the model.

In chapter 5 results are discussed and further work proposed. Finally, conclusions are given in chapter 6.

Chapter 2

Theoretical background

2.1 Energy in the wind

From a physical point of view, wind energy is the kinetic energy of the wind,

$$\frac{1}{2}mV^2, \tag{2.1}$$

were m is in kilograms and V is in m/s. Wind power is the conversion of this energy into a useful form like electricity, mechanical power (wind mills) or by using sails to propel a boat.

The kinetic energy in a certain volume of moving air (wind) can be calculated using Figure 2.1 [Boyle, 2004]. The volume of the air passing through the cylinder each second will be $10m \times 100m^2 = 1000m^3$. Multiplying with air density ρ gives the mass passing through the cylinder each second, which can be expressed as air density $\times$ area $\times$ velocity, i.e. $m = \rho AV$. Substituting for m in Equation 2.1 gives the kinetic energy in the wind per second, where ρ is in kgm/s, A is in m^2 and V is in m/s. The power of the wind P given in Watts (joules per second) can then be expressed as

$$P_W = 0.5\rho AV^3 \tag{2.2}$$

This is the power available in the wind for a wind turbine to use. As seen from Equation 2.2 the mechanical power will depend on the density of air, ρ, the area considered, A, but most of all the wind speed, V. A doubling of the wind speed will increase the power 8 times. Air density in higher elevations in mountainous areas is lower than average, but the average density in cold climates may be up to

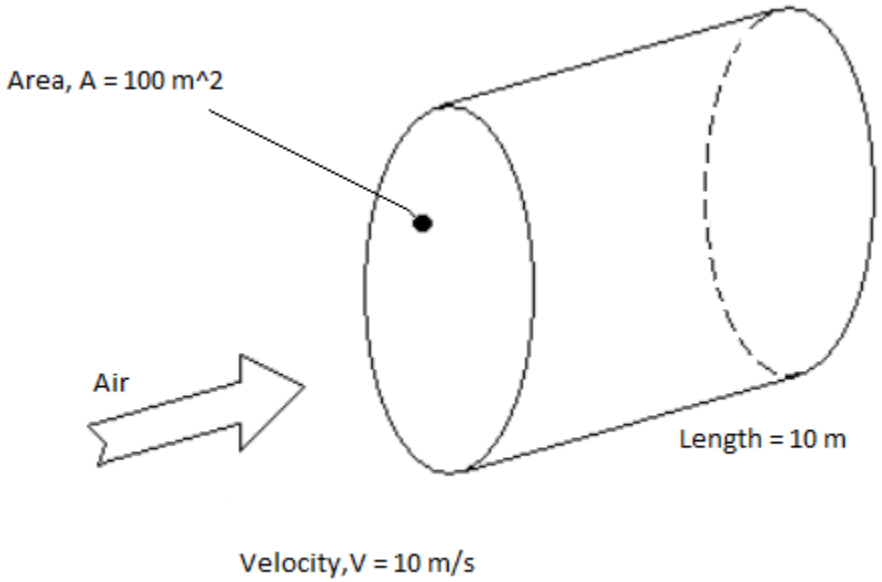

Figure 2.1: Cylindrical volume of air passing at velocity V, 10 m/s through a circular area A, each second.

10% higher [Boyle, 2004]. In cold regions overproduction up to 16% is recorded, due to higher airdensity and also airfoil modifications related to icing conditions [Jasinski et al., 1998]. This means placing wind turbines in cold areas will initially give expectations of a higher output. Considering the exposure to atmospheric icing the total production will normally be lower than average even though.

Figure 2.2 shows a typical power curve for a wind turbine. The Output power is given as a function of the wind speed.

2.1.1 How wind turbines extract energy

Wind turbines extract energy by slowing down the wind. Simply explained, the wind hits the turbine blades and the energy makes the blades rotate. For a wind turbine to be 100% efficient it would need to transfer 100% of the wind energy to electrical energy. This is not possible because of physical laws. Air blowing into a wind power station has to pass through the rotors, otherwise the air would pile up and increase the density of the air until preassure forces become unrealistic high. So the air must have energy left for blowing away. Due to this, the maximum limit of energy which can be extracted is found to be 0.59. This is known as the Betz limit [Manwell et al., 2002] and states that no wind turbine can possibly convert

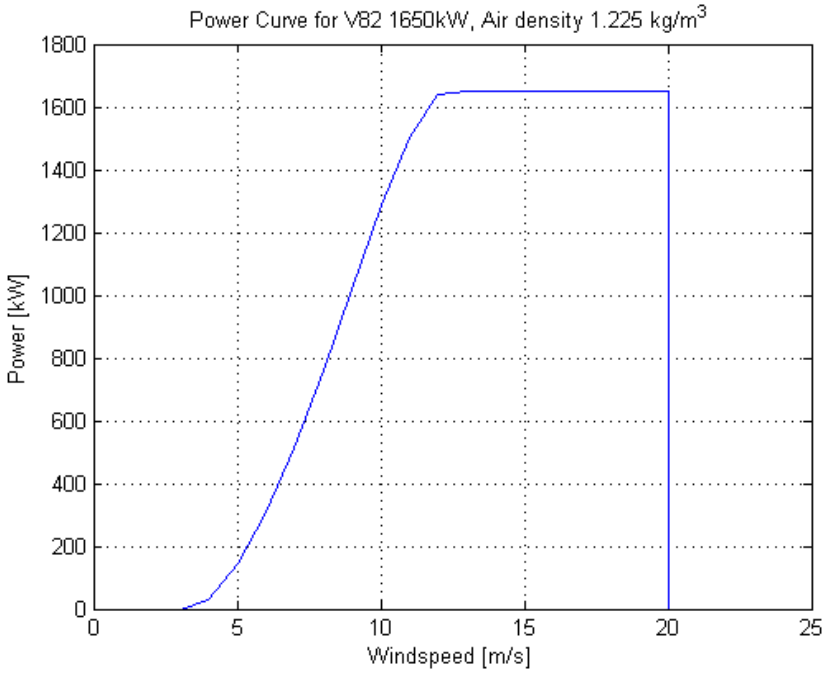

Figure 2.2: Typical Wind Turbine Power Curve

more than 59% of the energy in the wind. A turbine normally have an efficiency factor which is lower than 0.59, C_p is the constant used for this number which is the turbines efficiency or the power coefficient of the rotor.

The power produced by a wind turbine is then given by the equation:

$$P = P_w C_p \tag{2.3}$$

Where P_w comes from Equation 2.2 and C_p has, as mentioned, a maximum value of 0.59. Modern three-bladed wind turbines normally have a C_p ranging between 0.4 and 0.5 as friction forces in the rotor or axle shaft will decrease a turbine‘s efficiency even further.

For a given wind speed, the turbine efficiency C_p is a function of the tip speed ratio λ [Boyle, 2004]. This is defined as the ratio between the speed of the tip of the blades and the wind speed:

$$\lambda = \frac{V_{tip}}{V_{wind}} = \frac{\omega R}{V_{wind}} \tag{2.4}$$

where V_{tip} is the speed of the blades tip, V_{wind} is the wind speed, ω is the rotational speed of the rotor and R is the radius of the rotor. An optimum tip speed ratio is where the turbine operates most efficiently. At lower speeds some wind travel through the rotors without being converted to mechanical energy. If the tip speed ratio is to high, the turbine offers too much resistance to the wind, pushing it around the blades and not extracting the energy.

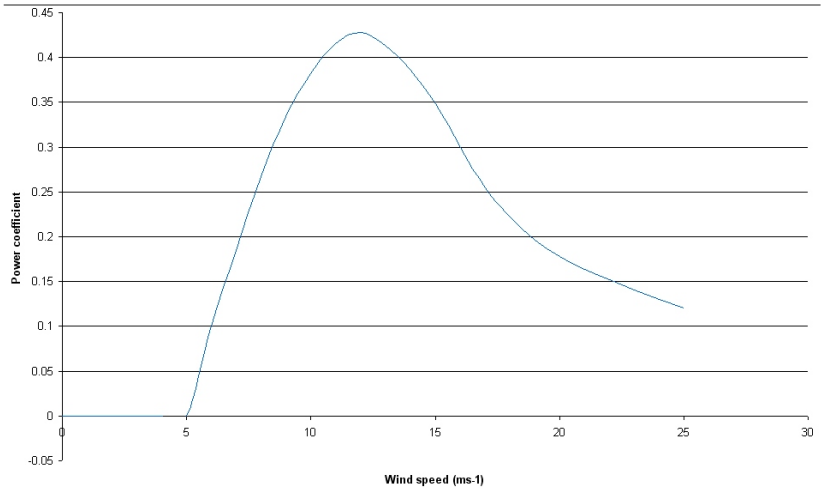

Figure 2.3: Power Coefficient as a function of Tip Speed Ratio

Figure 2.3 Shows the efficiency of a rotor as a function of tip speed ratio. The efficiency of the turbine is differing as the windspeed changes. Because of this, turbines developed for low wind speed areas have a different C_p curve than turbines build for high wind speed areas. The goal is to get as much energy from the wind as possible in the actual wind climate.

2.2 The turbine

The typical wind turbine used in power production today is a three bladed horisontal axed turbine (HAWT). Many companies provide the turbines(Vestas, Sinovel, General electric, Enercon and more). A typically build of a turbine is described in this section, based on information from the book Wind enrgy explained; Theory, Design and application, [Manwell et al., 2002].

A wind turbine exist of a tower, blades and nacelle including transformer, generator and control system. The turbine will produce electrical power for wind speeds ranging between approximately 4 and 25 $m\ s^{-1}$ depending somewhat on the type of turbine. At higher wind speeds the blades are locked to not damage the turbine itself. At wind speeds lower than the 4 $m\ s^{-1}$ the kinetic energy is not sufficient to drive the generator. Figure 2.4 shows a typiccal three bladed horisontal axed turbine with it's main parts.

Rotor is considered the most important component of the wind turbine. It includes blades and hub.

The "'Drive Train"' consists of the turbine's other rotating parts; they bring the rotation from the rotor to the generator. This normally includes a low-speed shaft from the rotor to the gearbox, and a high-speed shaft from the gearbox to the generator. The gear converts the slow rotation from the blades to more speedy rotation to drive the generator.

The generator converts the mechanical energy to electrical energy. Most turbines use induction or synchronous generators.

Nacelle includes the wind turbine housing which cover and protects content from the weather.

The Yaw-system controls the blades orientation so that the turbine can use the wind as efficient as possible. The productions is optimal when the blades are oriented 90^oC on the wind.

Tower and foundation is what holds the blades and nacelle. Hight of the tower is normally 2-3 times the radius of the rotor. There is normally a ladder on the inside of the tower giving access to the parts in the nacelle for maintenance work.

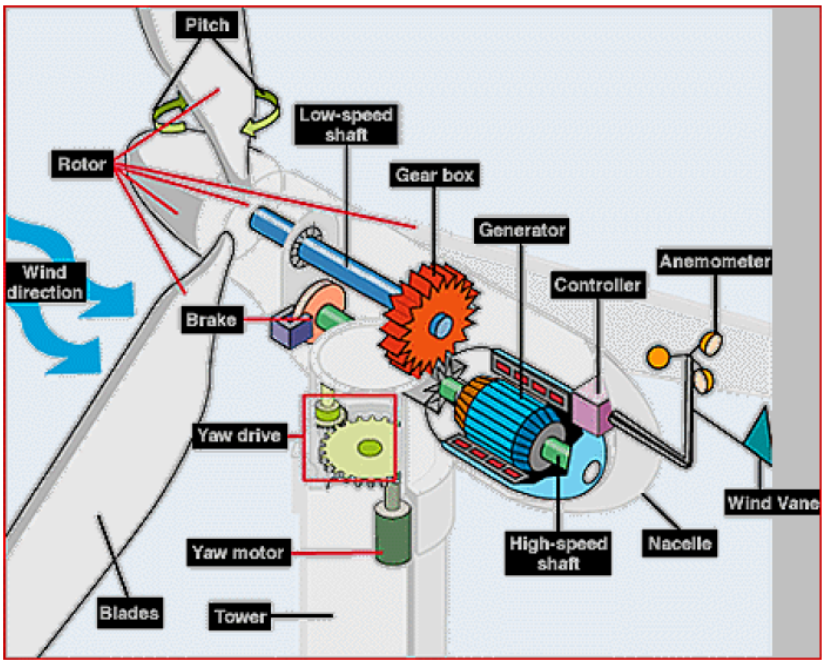

Figure 2.4: Typical build up of a Wind Turbine

The basement is solid and well anchored in the ground to keep the whole wind turbine stable.

Control system, this should maximize the energy production and protect the machinery from damage due to overloads and fatigue fractures by controlling speed, rotation, temperature and voltage. There are different types of control systems for controlling the speed of rotation and preassure on the blades. The most common are stall control and pitch control or active stall control which is a combination of the two. Stall control is a technology where the blades slightly twist as the wind and preassure gets to high using no active regulation. The design of the blades make them twist by them selfs when preassure gets to high. This creates a stall effect so that the preassure on the blades decrease. Pitch regulation works by twisting the whole blade from it's connection point using a motor. For low wind speeds the blades are pitched to achieve maximum output. As the wind speed increases, the blades are turned (pitched) in such a way that more wind passes through without affecting the wing. This gives less preassure on the wing and also less power.

The electrical system of a turbine includes cables, switchgear, transformers, yaw and pitch motors and other components needed to run the turbines electrical parts.

2.3 Aerodynamics

A Turbine wing works as an airplane wing and will in principal have the same lift and drag forces. The lift is often solely explained by saying that the air travels a longer path on the upper side of the wing than the lower side. This is called the Bernoulli effect. The effect creates a force from the high preassure region to the low preassure region. This force increases with the wind speed. For an airplane, we will use the term relative wind speed, which is the speed of the air relative to the wind speed. When this speed is strong enough, it will lift the airplane. Usually, wind tunnel experiments is used to design optimal wind profiles. Any deviation from this, as for instance covering part of the wing with ice, will reduce the lift force, and thus, the effect of a wind turbine.

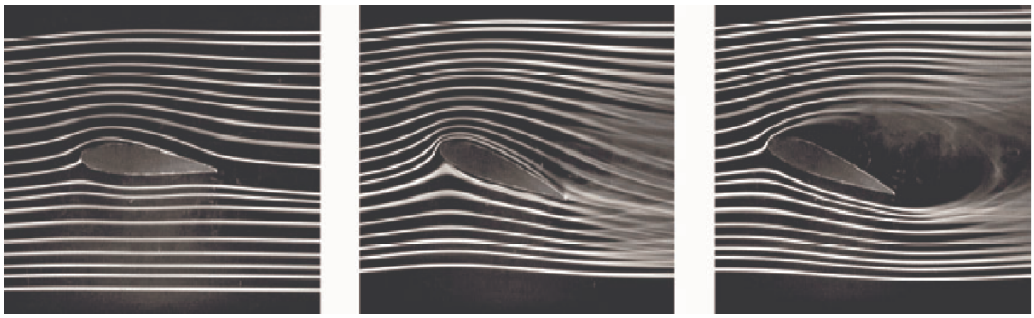

Figure 2.5: The images show an airfoil at different angles of attack. Farthest left giving the smallest lift, middle shows large lift and to the right the angle of attack is increased to a point where a stall effect is reached. Figure from [Babinsky, 2003]

2.4 Atmospheric ice

2.4.1 Meteorology

In the atmosphere there are processes like condensation, evaporation and forming of droplets and ice crystals continually. The sun heats the earth's surface unevenly and warmer air has a lower density than cooler air. Cooler air will therefore sink and take the place of the air that has been warmed up. The warmer air rises and cools. This convection process runs itself from hemispheric circulations to local airflows. Humidity in the air and differences in temperature decides whether this convection will form condensation, ice crystals, evaporation, rain clouds, super cooled droplets and so on.

When moist air is cooled, the air will reach a point where it becomes saturated

with vapor and droplets will start forming as the vapor condensates. This requires a condensating nuclei (CCN) where the particles can condensate. Particles are also required for ice crystals to form as the water droplets are further cooled and reach freezing level (0^oC). If such particles are not present, the droplets may be super-cooled and will then freeze immediately when impinging on an object [Salby, 1996].

2.4.2 How do atmospheric icing occur?

Definition of Icing: In general, any deposit or coating of ice on an object, caused by the impingement and freezing of liquid (usually super-cooled) hydrometeors. The two basic types of icing are rime and glaze [NSIDC, 2008].

Different types of Atmospheric icing

Atmosphric icing can be divided in two groups:

- Ice from precipitation (wet snow, freezing rain or drizzle).
- In-cloud icing (super cooled cloud droplets, temperatures below 0^oC).
- Hoar frost (Direct phase transition from vapor to ice. Low density ice which is normally neglected when it comes to loads of ice on structures [Makkonen, 1984].

Freezing rain or drizzle occurs when hot air aloft melts snow crystals and form raindrops. These raindrops fall through a freezing airlayer near the ground. Temperature inversions like this may occur in connection with warm fronts or in valleys where cold air is trapped below warmer air aloft [ISO12494, 2001].

Wet snow can form ice when the meteorological conditions allow it. In wet snow there is free water in the partly melted snow crystals. This water make the crystals able to adhere to the surface of an object. This happens when the temperature is just above the freezing point. If the temperature then decreases the accumulated snow will freeze and create ice [ISO12494, 2001].

In-cloud icing: A cloud droplet can be cooled below its actual freezing point due to lack of freezing particles, and usually be supercooled. When a super cooled droplet hits an object e.g. a power line or a wind turbine, the droplet freezes. Depending on the water flux this freezing will be either wet or dry. Dry freezing is when the droplet hits an object and freezes before the next impinges. This freezing will form rime, see figure 2.7 and table 2.1. If the water flux increases the droplets do not have time to freeze before the next impinges. This will create

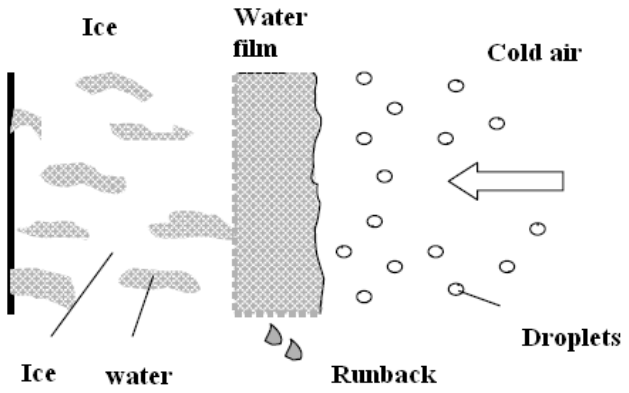

Figure 2.6: Wet growth of ice produce Glaze

a wet surface where the freezing occurs, see figure 2.6 and table 2.1. Wet freezing always produce glaze ice [ISO12494, 2001].

Freezing processes

When a droplet hits a surface, the droplet may freeze immediately (dry deposition), freeze after some time (wet deposition), or not freeze at all, and instead give contribution to old ice melting or shedding. The result depends on the energy budget at the surface. Primarily the budget is the sum of latent heat by freezing, sensible heat which is positive for air temperature above surface temperature, and net radiation. The budget also includes some minor terms like kinetic energy. If the energy budget is clearly negative, we have dry deposition; if it is clearly positive, ice shedding; in between we have wet deposition. Dry deposition leave an opaque, less dense ice flag towards the wind direction, while wet deposition leads to a dense ice, more uniform distributed. Ice shedding typically happens when there are positive temperatures, or by strong solar radiation. Increase in wind speed will increase the water flux and therefore increase the rate of icing.

Different types of ice

The ice accreting on structures is normally referred to as glaze ice, wet snow and rime. Which type of ice is created depends on the meteorological conditions when the icing occurs. The different types of ice are summarized in table 2.1.

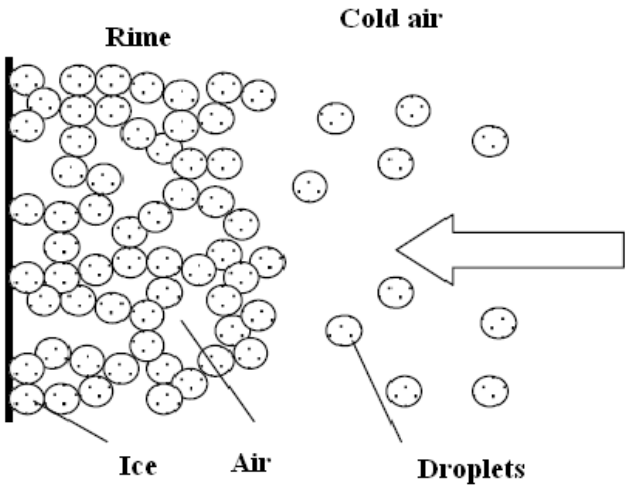

Figure 2.7: Dry growth of ice produce Rime

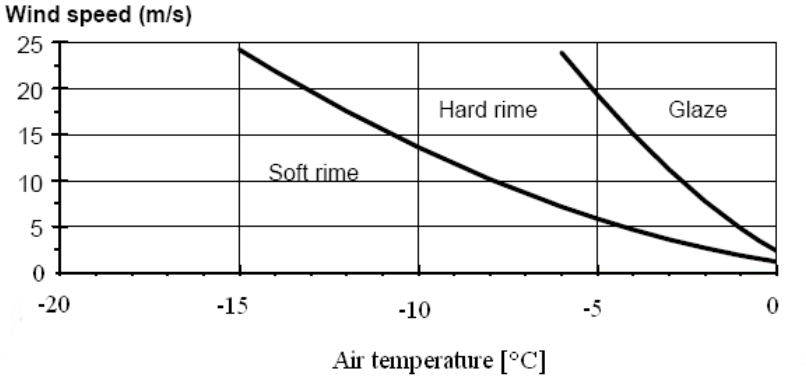

Figure 2.8: Influence of windspeed and temperature on types of icing (after [ISO12494, 2001])

Type of Ice	Density[kg/m^3]	Adhesion and Cohesion	Colour	Shape
Glaze	900	strong	transparent	evenly distributed/icicles
wet snow	300-600	weak/strong	white	evenly distributed/eccentric
Hard rime	600-900	strong	opaque	eccentric, pointed windward
soft rime	200-600	low to medium	white	eccentric, pointed windward

Table 2.1: Ice classification

Table 2.1 show that hard rime has a density of 600-900 kg m^{-3}. In practice hard rime is considered to have an average density of 500 kg m^{-3}.

Glaze

Glaze is the highest density ice. Freezing conditions are always wet and glaze can be formed from both precipitation icing (freezing rain or drizzle) and in-cloud icing. Temperatures during the freezing process are close to 0^oC but can vary some with varying wind speed, see Figure 2.8. When a droplet hits the accreting object, part of the droplet freezes immediately, the rest is spread over a larger surface before freezing [Makkonen, 1987]. The water which does not freeze at once will make up the wet freezing surface. The spreading of the impinging droplet and the wet freezing surface will not allow air to be trapped within the ice. This gives glaze its high density.The accretion rate of glaze ice varies mainly with rate of precipitation, wind speed and air temperature [Makkonen, 1987, Makkonen, 1996].

Figure 2.9: Glaze ice formed on a grass

Rime

Rime has a lower density, is more porous and a lot weaker than glaze ice. When rime is formed the whole drop freezes almost immediately when impinging. The droplet is not spread out and keeps its original shape. Due to the rounded shape of the droplets, air can get trapped in between the impinging droplets as shown in

figure 2.7. Rime can be divided into soft rime and hard rime. If the water vapour is deposited by first condensating on the surface, and then freeze immediately after, it is soft rime. This process may be very fast and leave the surface slippery.

Hard rime is normally a result of in-cloud icing. Mountains covered in clouds are typical examples where hard rime will form. In-cloud icing will often be a mixture between wet and dry freezing, ice formed this way is normally referred to as hard rime. Super-cooled droplets in the clouds hit the mountain sides (or a structure like a wind turbine or TV-mast standing on top of the mountain). The droplets freeze when impinging on the surface. Depending on mostly temperature and wind speed, the freezing will be dry causing rime or wet causing glaze. The combination of dry and wet freezing is, as mentioned, referred to as hard rime. In practice, in-cloud ice is a mixing of hard and soft rime, and the density vary a lot, but typical values are between 300 to 700 kg m^{-3} [Knut Harstveit, pers. comm.]. In ISO (12494) a typical value of 500 kg m^{-3} is recommended if more information is not available. This type of icing is the most common for wind turbines. On-shore turbines are typically placed on top of mountains exposed to wind (of course) and clouds. Off-shore turbines will also be very exposed to incloud-icing when fog is forming on the ocean.

Wet Snow

Wet snow is partly melted snow crystals and are therefore existing when the temperature is above freezing level. Wet snow ice is formed when the partly melted snow lands (or blows onto) an object, sticks and freezes due to a drop in temperature [ISO12494, 2001]. Newly formed ice from wet snow will contain unfrozen parts and therefore be weaker. At lower temperatures and as time goes (as long as the temperature is below freezing level) larger portions of the wet snow will freeze and the ice becomes stronger.

Topographic Influence

Mountains, valleys, oceans, lakes, all topography has an influence on the movement of air. Formation of clouds happens when air is lifted and cooled. This process is reversed when air is sinking and warmed up; snow crystals melt and water droplets evaporate.

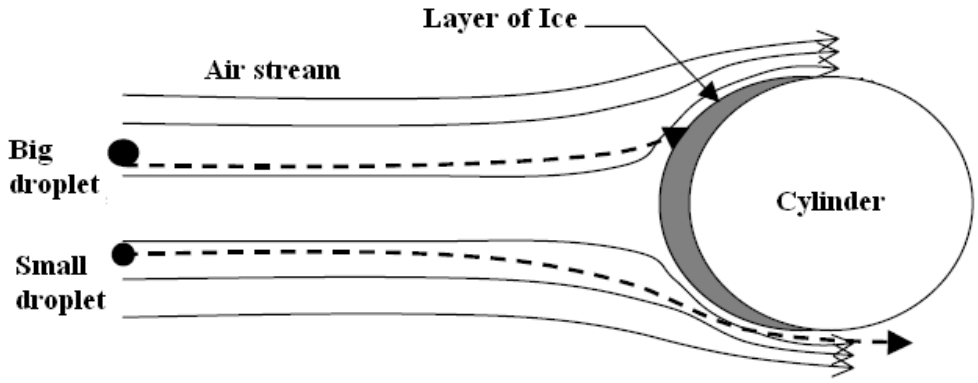

Figure 2.10: Air streamlines and Droplet Trajectories around a cylindrical object (after [ISO12494, 2001])

2.4.3 Droplet trajectories and dimension of structures

The size and numbers of droplets hitting an accreting object is of high importance to the buildup of ice. Investigation of the collision efficiency, that is the number of droplets hitting an object related to the total number of incoming droplets, has been studied. Investigation of droplet trajectories around a cylindrical object show that bigger droplets are more likely to hit an object then small droplets [Langmuir and Blodgett, 1960]. As shown i figure 2.10 air streamlines are created around an object as the air flows on the sides. Droplets transported by the wind will normally follow the air streamlines. When the streamlines approaches an object they are bent off. Bigger droplets have a larger mass and higher inertia and therefore will not be influenced as much by the air streamlines around the object (Figure 2.10) Air masses containing large droplets will therefore give a high collision efficiency compared to air masses containing small droplets.

For given meteorological conditions, icing will vary with dimension and shape of the accreting structure as well as droplet size. The wind exposure of the structure is also important; ice normally builds on the windward side of an object. Due to the droplets inertia, the collision efficiency is larger for small objects. The streamlines for droplets will deviate from those of the air. Passing a thin object, the air streamlines will change very little, and therefore droplets will mostly go straight on the thin objects. Passing a bigger (wider) object, the air streamlines changes significantly and also the droplets are forced around the object. The collision effi-

ciency is then decreasing for bigger objects. For this reason icing on structures is observed on corners, rims, sharp edges etc. Smaller objects like power lines, antennas, turbine blades (specially the edges) are also exposed to significant accretion of ice compared to larger "'one dimensional"' structures [ISO12494, 2001].

For wind turbines, it has been shown by [Virk et al., 2010] through numerical analyses that an increase in blade profile size reduces the dry rime ice accretion on the leading edge. This goes very well with the droplet trajectories following streamlines around large objects and deviating from the streamlines around thin objects and therefore hitting them.

2.5 Ice on rotors

When ice accrete on the blades of a wind turbine, the turbine apparently functions as normal, the blades may turn and energy is converted, though the turbines performance is lowered. For the wind industry, the effect of icing on turbine blades has been studied more during the last 5 years. Power loss due to icing has been estimated to 17% to 25% for one year by e.g. [Homola et al., 2009, Øyvind Byrkjedal, 2009].

Most of the knowledge of the aerodynamics of a wing is established through airplane industry. The effect of ice on aircraft wings is well documented using wind tunnels [Broeren et al., 2006]) and numerical simulations [Bragg et al., 2007]). Experimental methods has been developed further to determine the effect on turbine blades. In 2001 a numerical model of ice accretion on wind turbines was presented [Makkonen et al., 2001]. The model shows how ice is accreted on the tip of the blade, on the blades leading edge. The leading edge is always catching most ice due to droplets collision efficiency; The more droplets that hit the object, the more droplets will imping and freeze, and the leading edge will always have the ability to hit the most droplets as explained in 2.4.3.

Ice accreting on airfoils has a detrimental effect on the wing's aerodynamic performance. This is mainly caused by a change in the flow behavior when ice is present. [Virk et al., 2010] did a research on the effect of ice accretion on turbine blades. They found that the leading edge catching ice first of all gives a reduced torque which changes the capability of the turbine to utilize the energy in the wind. The aerodynamic changes on a turbine blade can be written as

$$F_y = (C_L sin\phi - C_D cos\phi)\frac{1}{2}\rho W^2 c(r) \tag{2.5}$$

When analysing the wind turbines capability to produce power, the change in

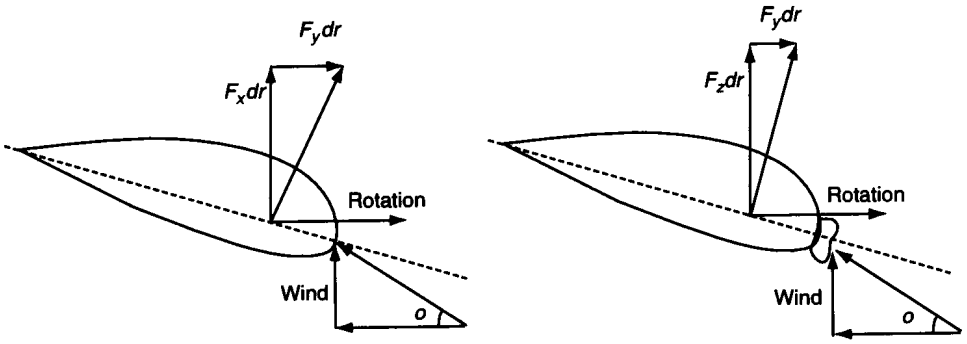

Figure 2.11: Wind turbine profiles with and without ice illustrating the reduced torque in case of leading edge accretion. Figure from [Virk et al., 2010].

torque coefficient is quite important and can be expressed as

$$C_y = (C_L sin\phi - C_D cos\phi) \tag{2.6}$$

where ρ is the angle between the plane of rotation and the relative air velocity [Virk et al., 2010]. This is mainly influenced by the ice accreting at the leading edge as shown in Figure 2.11.

In 2009, a study on the effect of ice shapes on a turbine blade was performed by [Barber et al., 2009]. Ice shapes were produced and placed on a turbine wing. Shapes, orientation and geometry of the ice shapes were based on in-situ measurements, photographs and numerical modeling. The result shows that the tip speed ratio is decreasing for ice covered blades. It also shows that larger ice cover gives lower power output. The lower efficiency may be due to more of the wing being covered by ice; The tip of the wing will cover first, especially the leading edge, then the ice flag increases, and also cover more and more of the wing as long as the icing event lasts.

A study, [Seifert and Richert, 1998], also shows an increase in drag coefficient and corresponding reduction in power production. Seifert calculated the reduction of performance for different ice shapes for a fictitious turbine. The resulting power curves are shown in Figure 2.12.

The quality and shape of the ice has, according to Seifert, a significant influence on the performance. As Seifert describes, different shapes can reduce the performance less even if the icing covers a larger part of the blade. This is shown by the power curve where 44% of the blade is covered. The reduce in power is less here compared to when 22% of the blade is covered. This is due to the different quality and shape

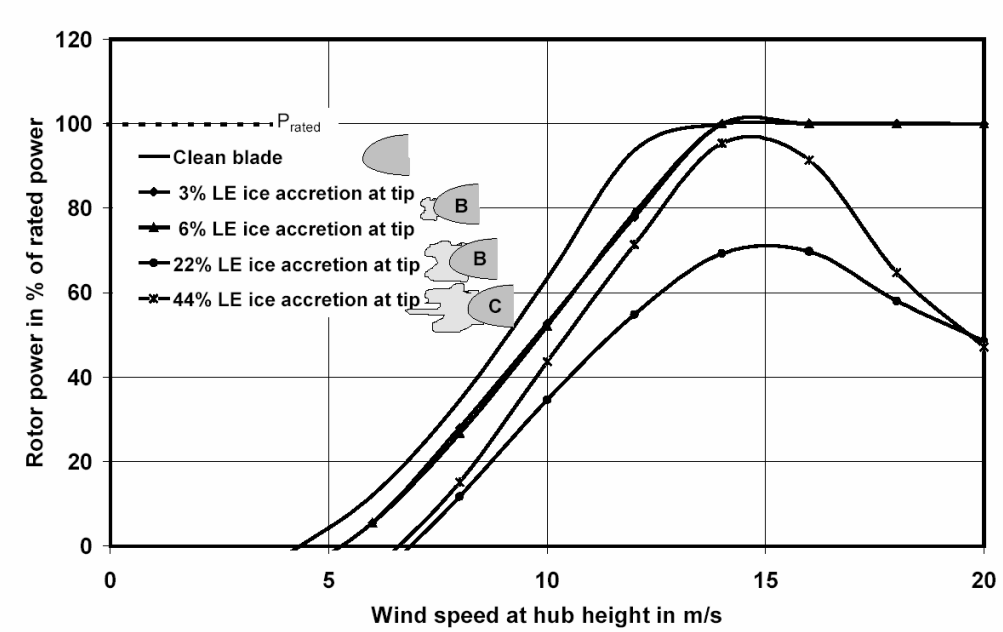

Figure 2.12: Calculated power curve for a pitch controlled factious turbine with different types of ice accretion. picture form [Seifert, 1998]

of the ice. In this thesis, no knowledge of the quality or shape of the accreting ice is known and the load is the only measure which tells one icing event apart from another.

Chapter 3

Data basis and methods

Aapua wind farm is located in northern Sweden and is the northernmost wind farm in Sweden. All together 7 turbines with a total stated power of 9.9 MW are installed at the site and production started in 2005. The turbines are of type Vestas V82-1650kW Arctic, scaled down to 1500kW from the original 1650kW to better function in arctic climate [Vestas, 2008]. The cut-in and cut-off speed is set to 3.5 m/sec and 20 m/sec, respectively. The re-cut-in speed is set to 18m/sec to avoid to high frequency of start and stops. The power curve for the turbine can be seen in Figure 2.2. Each unit has a nacelle height of 78 m and a rotor diameter of 82 m. The turbines are equipped with special functions as heated anemometer and nacelle to be able to operate in cold climate. Temperatures at Aapua may come down to -30 C during winter season. Winds tend to be stable and seldom higher than 10 m/s. The wind turbines used are especially designed for low wind speeds and have a higher output for low winds than other turbines. Total production at Aapua is approximately 30.1 GWh per year, which corresponds to the electricity needs of 6.000 houses [Siral, 2005].

An ISO standard was developed during a period from 1989-2001 [ISO12494, 2001]. This was a major task in developing a standard for use in technical projects concerning the issue of atmospheric icing. The standard describes measuring equipment and procedures recommended for measuring and calculating ice loads and icing events at sites or on structures. The equipment and measuring techniques used at Aapua are according to this standard.

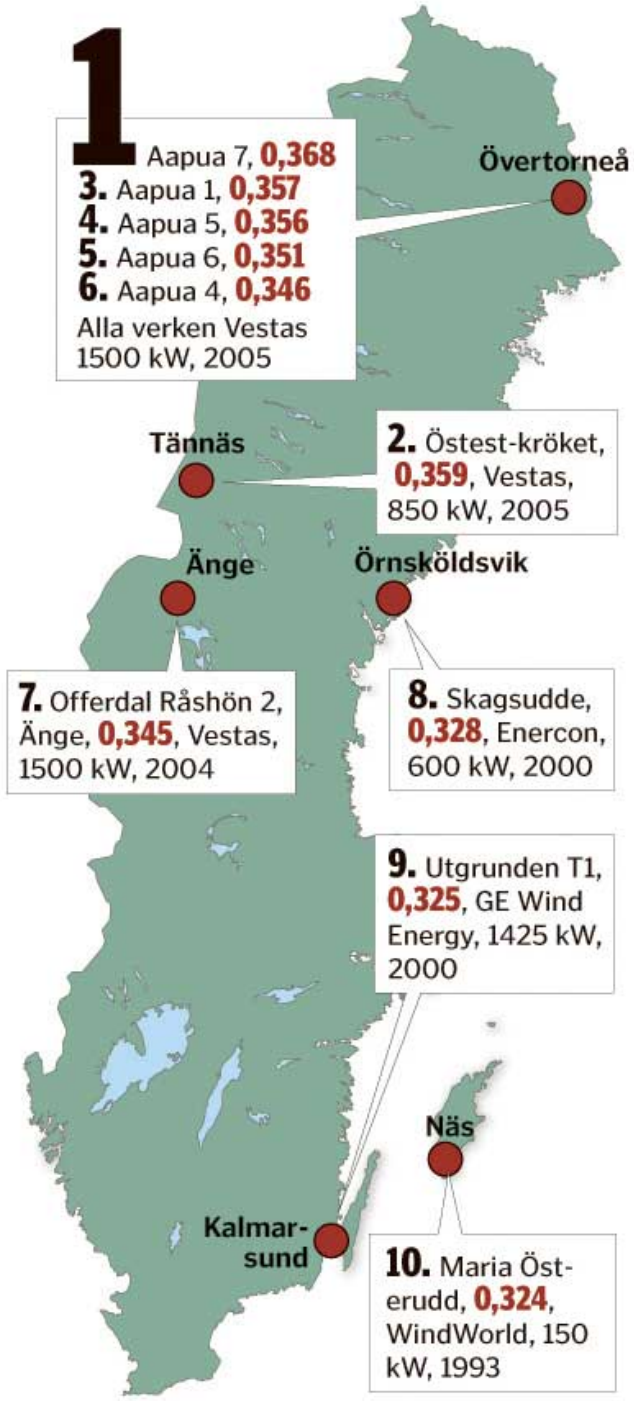

Figure 3.1: Map showing different wind farms in sweden. Aapua is the northenmost wind farm located close to Övertorneå in northwest Sweden.

3.1 Measuring equipment and data collection

Ice load measurements $I(t)$ are done with a Saab Ice Monitor, a vertical steel rod with a length of half a meter and a diameter of 30 mm. There is a load cell at the bottom end of the pole measuring the vertical load. The rod is free to rotate in the wind and ice is therefore thought to distribute fairly even on all sides of the pole keeping its cylindrical shape. The surface will get somewhat rougher as ice is accreting, still the airflow is assumed to bend as for a perfectly shaped cylinder.

Figure 3.2: An ice load measuring stick. The ice is distributed around the whole rod keeping a somewhat cylindrical shape [Drage, 2005].

Icing rates d(I) are observed using a Holo Optics T41 ice sensor. The ice accreting on the instrument is melted immediately after registration, and therefore icing rates can be measured continuously. The Holo Optics T41 is made to be mounted on wind power stations. At Aapua wind farm, the Holo Optics T41 was upgraded 7th December 2009 to a version with higher heating capacity. As the heat in the former version was not sufficient, there can be errors in the data before this time.

Each turbine is equipped with 2 anemometers measuring the wind speed V(t). These are heated to avoid errors due to ice. Anemometers are the eyes and

ears of a turbine, and need to be reliable in all weather conditions. Developing reliable anemometers has been given a lot of attention [Tammelin et al., 1998, Homola et al., 2009, Parent and Ilinca, 2011]. The recorded wind speed data is set to the average wind speed during a ten-minute period.

Wind vanes are used to measure the direction of the wind. This measurement is needed to automatically rotate the turbine against the wind at all times. Wind direction can also be used to observe from which wind direction icing is most severe. The use of wind vanes to identify icing events has been proposed [Tallhaug, 2003]

Other standard meteorological data were collected including air humidity, air density, air preassure and visibility. All data are recorded in ten-minute intervals giving one value each ten minute. This value is then stored in a database. Notation is shown in Table 3.1

Observed value	Parameters name
Temperature $[^oC]$	$T(t)$
Wind speed $[m/s]$	$V(t)$
ice load $[N/0.5m]$	$I(t)$
Wind direction $[360^o]$	$\alpha(t)$
Power $[kWh]$	$P(t)$
Air Density $[kg/m^3]$	$\rho(t)$

Table 3.1: Table giving the names of each parameter.

Meteorological data is recorded on all 7 turbines. Ice load and icing rates are only measured at one location and will therefore have the same values for all turbines. It has been shown that only small deviation in height and location for an ice sensor will alter the ice accretion rates [Homola et al., 2006]. Ice sensor and ice load weight is placed close to turbine 7, no measurements are done on the rotor blades or turbine itself. The icing rates and ice loads measured are thus not identical to the ice loads and rates of accreting ice on the turbine blades. Still, the measurements are considered the best indicator of icing events and their severity at the site with todays equipment.

3.2 Data cleaning

All turbines are equipped with alarms. Alarms are triggered for several reasons, typically malfunctions like frozen anemometers, frozen wind vanes, power cut and control system failure. Data analysis started with removing periods where the turbine had triggered an alarm code. To be able to calculate loss, a power curve defining expected output power for the turbine type at Aapua was found. This

curve is calculated from observations done in October and November in 2009 when temperature was above 2^0C. All deviation from an expected power curve is considered to be loss, and all loss calculated after data cleaning is considered to be loss due to icing.

When an anemometer is frozen, it results in what is recorded as overproduction. This is because a frozen anemometer shows a lower wind speed than the real velocity. The expected output is based on the wind speed measured by the anemometer. Generated power will then show a higher value than expected output. To exclude observations done with broken or frozen anemometers, an upper limit based on the expected power is calculated using the standard deviation for different wind speeds. The limit is made by fitting a curve corresponding to output 8 standard deviations higher than expected for low wind speeds, decreasing to two standard deviations for high wind speeds. The reason for the rather large deviation from the expected power during low wind speeds are the non-linear start and stop at cut-in wind speed, [Homola et al., 2009]. In literature, overproduction due to airfoil modifications and change in air density is observed up to 16% [Jasinski et al., 1998]. The result can be seen in Figure 4.1.

The main anemometer on turbine 4 was destroyed early in the season 2009 and therefore the wind measurements are not reliable. Power output showing very high values for almost no wind were observed and the breakdown of the anemometer was discovered by comparing the wind speed values to those obtained on the other turbines. The second anemometer on turbine 4 only show data for a few weeks and is therefore not considered a reliable backup. The data from turbine number 4 is thus sparse and not used in further analysis.

To be able to extract information, obvious errors in the recording of the data were eliminated. Examples are different parameters showing a value of -999,9. The temperature, wind speed, air pressure or air humidity can never possibly reach this limit and numbers are put to "'not a number"' (NaN) and ignored during analysis. Only the NaN value is ignored and other parameters measured during the same period may be used. This is done to lose as little data as possible. Where more than one parameter is needed to do an analysis, example wind and ice, both values are ignored if one of them already is put to NaN.

3.3 Data analysis

3.3.1 Power output model

A power curve $\hat{P}(V)$ for the expected output value for the turbines is made using measured data from the wind farm where temperatures are above 2^oC,

as described over. The expected power output is also named "'no ice"'. Loss in power output is defined as everything deviating from the expected output value for the wind turbine. Power produced at a specific winds peed will vary as the air density varies. This does result in negative loss (overproduction) when power output deviates from the power curve $\hat{P}(V)$ by producing more power than expected.

Power losses during the winter season are quantified by summing the deviations from the expected value every month. The losses for every week are further used to investigate an icing event, and during what part of the icing event, the most severe loss is observed.

The relationship between ice load, wind speed and power output is the main attention in this study. To get an impression of how the data is distributed, the data is gathered in classes. The wind speed is divided in 20 classes with class 1 covering the wind speed from 0.5 to 1.5 m/s, class 2 from 1.5 to 2.5 m/s and so on. Ice load classes are divided as it seemed reasonable by a visual analysis of the clustering of the data. This made the following classes measured in kg/m: [-.4 0), [0 .4), [.4 1), [1 2), [2 4), [4 6) and [6 10]. The wind speed bins are plotted against ice load bins in Figure 3.3.

A basic model giving the power output $\hat{P}$ based on an observation (V,I) can be made by calculating the mean value of the power output within each box shown in Figure 3.3. Interpolating between the power values will then give the power, $\hat{P}$ for each observation of wind speed and ice load (V,I).

$$\hat{P}_{mean}(V_k, I_l) = \frac{1}{N} \sum_{V \in V_k} \sum_{I \in I_l} P(V, I) \tag{3.1}$$

where P(V,I) are the observation points in the boxes. The median can be used as another estimator of $\hat{P}(V, I)$ by calculating the median value instead of mean in eq. (3.1). The median value is often used to avoid the contribution of extreme out layers.

A model estimating power output,$\hat{P}(V, I)$, is developed based on the observation data from turbine number one. The performance of this model is then verified using the remaining turbines.

The energy output from a given wind turbine as function of the wind speed is known from the manufacturer. Icing will affect the power output of the turbine, but the changes are not well understood. Due to many factors, the geometry of the ice in each class will vary with corresponding variation in the power output function, and thus the energy function will vary. Given enough cases, a statistical curve may be found.

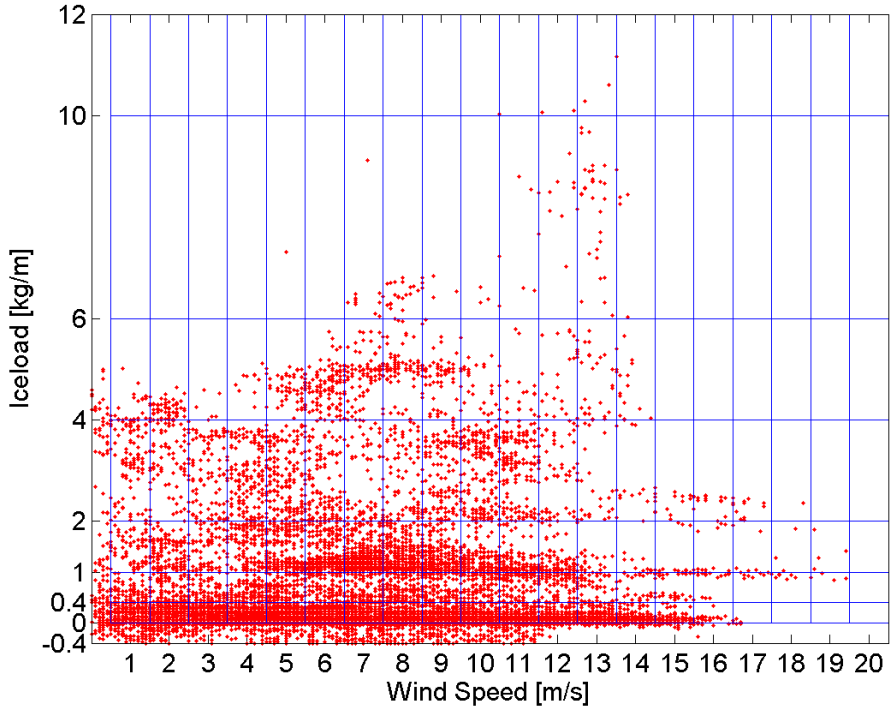

Figure 3.3: The grid shows how wind speed and ice load bins are distributed.

3.3.2 Bootstrap

Bootstrapping is a way of testing the reliability of a dataset $x[n]$, for $n = 1, 2, ...N$. This is done by creating pseudoreplicate datasets by resampling with replacement. The new datasets $x_m[n]$ are generated by randomly sampling the original character matrix to create M new matrices of the same size as the original [Efron, 1982]. In our case a mean value for the power output is found for every location $\theta = P^{mean}(V_k, I_l)$ in a grid or boxgrid from eq. (3.1), as seen in Figure 3.3 and Figure 3.4. And a measure of the variance,σ^2, of the mean, θ, is given by bootstrapping.

$$\sigma^2_{boot} = \frac{1}{M} \sum_{m=1}^{m} (\theta_m - \theta)^2 \tag{3.2}$$

Bootstrapping are preformed to find the variance, or standard deviations, for all power curve estimation methods in this these. If the original matrix contains a large number of points with little variation, the deviation will be small. With a smaller number of values (small N) and a large variety in the original matrix, the standard error is expected to be considerably larger.

For median estimates, the bootstrapping technique is somewhat special as the median consist of a single value from a set of data. Since replacement is used, it is possible that one sample is picked twice, and the new median number θ_m will most likely differ from the original.

According to [Huang, 1991] the bootstrap method overestimates the variance for the median in a discrete distribution. This is shown for an asymmetric Bernuolli distribution and considered to count also for other distributions like geometric and Poisson. Still bootstrapping is a well-known method used to estimate the variance of the median and according to [Ghosh et al., 1984] the bootstrap method gives a satisfactory result on random samples of a univariate distribution.

3.3.3 Kriging

Kriging is a geostatistical technique used to estimate the value of a random variable (Z) at an unobserved location (S_0) from observations of its value at nearby locations (S_{1-n}). Kriging produces a weighted average where each observed location is multiplied by a weight, λ, telling how much the value influences on the estimated value of the random variabel Z [Cressie, 1990]. Ordinary kriging assumes an unknown mean, μ. If the variable Z is observed at a number of locations giving values $Z(s_1), Z(s_2), ...Z(s_N)$, then the ordinary kriging method can be applied by

$$\hat{Z} = \sum_{i=1}^{N} \lambda_i Z(s_i) \tag{3.3}$$

where the weights are normalized [Cressie, 1990],

$$\sum_{i=1}^{n} \lambda_i = 1. \tag{3.4}$$

A typical example of a random variable is the elevation, z, of the landscape as a function of the geographic location. In this thesis the unobserved location is a point in a preset grid (V, I) obtained from wind speed and ice load and the estimated variable is the power output of a wind turbine, P. The nearby locations are the observed values of power from the turbines for the wind speeds and ice loads measured $P(V, I)$.

In a dataset of measured or observed data one can experience a non-uniform density distribution. Some parts of the dataset may have only few values if a specific event has occurred only few times. The linear distance between the points may be large, and using a defined box for which data points to include in the calculation, could cause the wanted value to be estimated from one or two points in extreme cases. In kriging, one can choose to always have a minimum of data points to calculate the wanted value. This may bias the result, but the bias is reduced by weighting the data points as a function of their linear distance, $d = \sqrt{|(V, I) - (V_k, I_l)|^2}$, to the location of the estimated value. The weight used here is

$$\lambda = \frac{\exp(\sum(x - x_0)^2)}{2 * 0.8} \tag{3.5}$$

where x is the observed point and x_0 is the grid point.

Figure 3.4 describes the kriging method where the red stars are the N=50 nearest point to the grid point (8,6) shown in green. The mean value of the red points weighted as a function of their distance to the grid point (8,6) will define the power output value for the particular location.

In our case the power output for each point in the preset grid shown in Figure 3.4 is estimated using the kriging method for ordinary kriging [Stein, 1999]. The points in the grid (V, I) is shown as blue stars in Figure 3.4. The stars have defined values of wind speed and ice load. From each point in the pre-set grid, the linear distance to all other points based on wind speed and ice loads are found. The weighted mean of the corresponding power output $P(V, I)$ from the

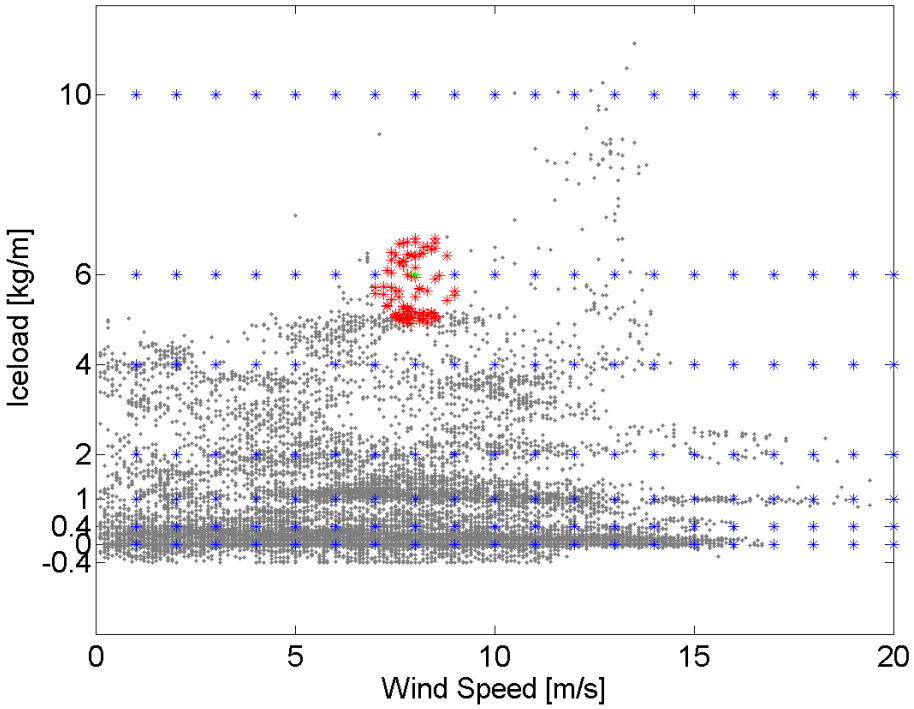

Figure 3.4: The preset data points used in Kriging is shown as blue stars. The gray dots are all data points from turbine 1 and the red points are the N=50 closest to the gridpoint of 8 m/s in wind speed and 6 kg/m in iceload.

nearest N=50 points is then chosen as the output value for the grid point (V, I). A model $\hat{P}_{krig}(V, I)$ is obtained based on the kriged values. Bootstrapping is used to calculate the variance and standard deviation of the estimator $\hat{P}_{krig}$.

3.3.4 Correlation

The correlation between output values obtained from models and observations is calculated using a standard equation for the correlation coefficient between two random variables.

$$Corr(x, y) = \frac{E[(X - \mu_x)(Y - \mu_y)]}{\sigma_x \sigma_y} \tag{3.6}$$

Where E is the expected value operator, μ_x and μ_y are the expected values of X and Y. σ_x and σ_y are the standard deviations [Stark and Woods, 2002]. Correlation is a measure of the linear relation between two variables, in this case the measured and modeled power output. The correlation will not tell how far the values are apart but rather how the values follow each other, and catches the dynamics in the datasets.

The Mean square error (MSE) is used to see which of the models have the closest values $\hat{P}$ to the measured power output P_{obs} The MSE is found by

$$MSE = \frac{(\hat{P} - P_{obs})^2}{N}, \tag{3.7}$$

where N is the number of data in P_{obs} and $\hat{P}$ [Stark and Woods, 2002].

The models are tested on data from all turbines, except turbine 4 and the modeled and expected ("no ice") outputs are compared to the measured output.

3.3.5 Evaluation of performance

After testing the models, their performance in means of correlation and MSE is evaluated. The model considered to perform best is then used in further investigation. Time series of modeled, expected ("'no ice"'), and measured ice are produced as well as time series for ice load and temperature. In cases where the different power output curves are not correlating well, temperature and ice load is examined to find a better understanding of the performance of the model. The processes which alter the efficiency of the turbine are investigated using the same method.

Chapter 4

Results

4.1 Data cleaning

Figure 4.1 illustrates cleaning of data. Wind speed is plotted against power output. The points shown in red, seems to give high production during low wind speed. The true wind speed is not measured due to frozen anemometers and the registrations are filtered out. The green line defines the border of power output considered possible. Output varies with air density and overproduction of 10% is normal in arctic regions due to high air density. There was no optimal power curve available from the manufacturer to calculate the 10% overproduction from. The green line is therefore estimated by investigating the output from all turbines and fitting a curve to the outer border of what is considered possible production for the turbine type at Aapua. All data containing alarm codes are also filtered out. This resulted in an average of 3000 data points removed from the measured 26000 for each turbine, which is approximately 10%.

Observations from turbine 1 are plotted as function of time in Figure 4.2. The red points are the points from Figure 4.1 which are eliminated. It can be seen that the observations are clustered in time, which is consistent with the thought that they are due to frozen or broken anemometers. If they were spread randomly, the output on small wind speeds could be thought to have other reasons. Within the first period there are two blue observations within the eliminated points. These may, as the red, show a too low wind speed but fall within the range of what is defined in this paper as possible overproduction and are included in calculations.

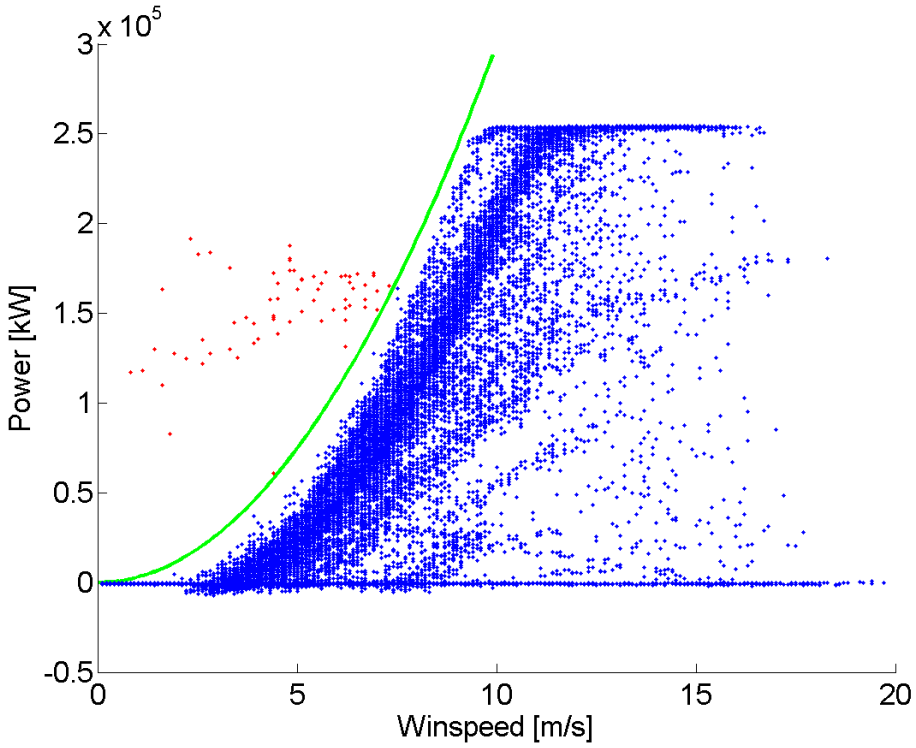

Figure 4.1: Observation data from turbine one from October 1st 2009 to March 31st 2010 is plotted with wind speed against power output. Blue points show data used further in analysis while red are outlayers filtered due to malfunctioning anemometers.

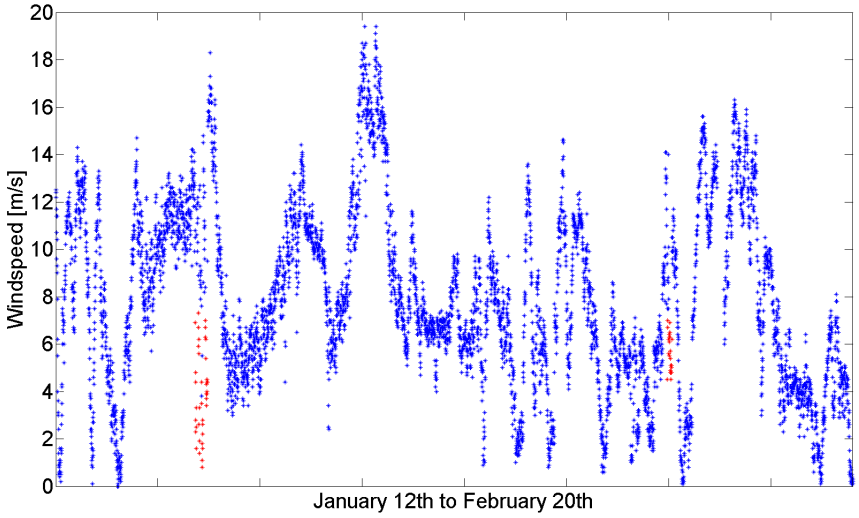

Figure 4.2: Observation data from turbine one is plotted with wind speed as a function of time. The red dots are the measurements falling outside the green line in the cleaned data.

4.2 Distribution of observations

In Figure 4.3 the red line show the power curve made for the turbine type at Aapua as explained in 3.2. It can be seen that measured output above rated power is somewhat higher than the expected. This will contribute to what is recorded as overproduction and therefore contribute to an underestimation of the total loss. The blue points are all observations from turbine number one after cleaning data. It can be seen that most data is clustered around the power curve. Some observations show lower power output and there is also observed zero output for all wind speeds up to 20 m/s. It should be noted that observations during high wind speeds mostly show zero in output.

4.3 The total production

An overview of the production and the calculated production loss at Aapua wind farm during the winter season 2009-2010 is given in Table 4.1. The measured and expected output is based on the cleaned data therefore all loss is considered to be due to icing. The total losses are significant and is shown as per cent of expected output power. It should be noted the severe loss during the months of November

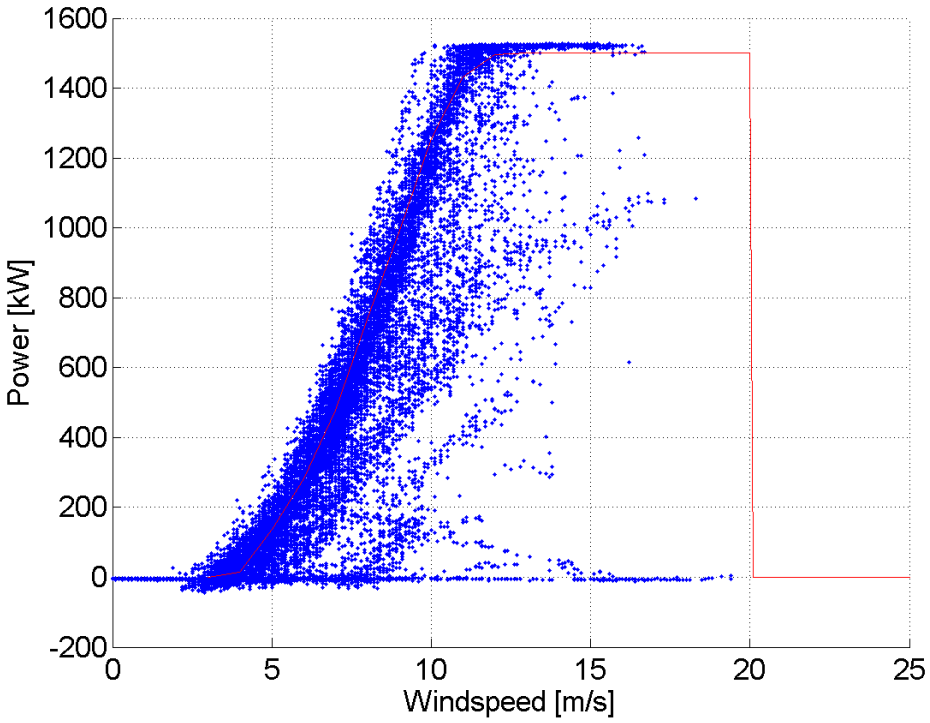

Figure 4.3: The distribution of measured data points after data cleaning from turbine number one is shown in blue and the expected power curve is shown in red.

	Observed [MWh]	Expected	Loss [%]	Ice load [kg/m]
October	7889	8753	9.9%	1720
November	6343	10200	37.8%	2968
December	10098	12570	12.3%	1515
January	5966	14342	52.5%	4752
February	9770	11993	18.5%	1215
Mars	15023	15902	5.5%	65
SUM	55088	73760	25.0%	-

Table 4.1: Key numbers for measured and expected production for the whole wind farm at Aapua. Losses are shown in per cent of expected output. Total ice load in the last column.

and January and the low loss in March. December is also a profitable month with low loss. The production is somewhat lower than in March, which can be explained by lack of data for 10 days from 21st to 31st of December. It should also be noted that March has a total measured ice load of 329, significantly lower than other months. The production loss due to ice for the wind farm as a whole is calculated to 25.0%.

-	Observed [MWh]	Expected	Loss [%]
October	10611	13021	18.5%
November	7019	12401	43.4%
December	10200	12064	15.4%
January	6338	14342	55.8%
February	9275	12683	26.9%
March	13592	16783	19.0%
SUM	57035	81294	29.8%

Table 4.2: Key numbers for the measured and expected production for the whole wind farm at Aapua. Expected and observed output is calculated from the original data and losses are shown in per cent of expected output.

The total loss calculated from the original data can be seen in Table 4.2. The original data is not cleaned and therefore include losses due to other reasons then icing. It is observed that losses increase for original data compared to cleaned data. The total loss is calculated to 30% which also shows that icing stands for more then 2/3 of the total loss.

4.4 Ice affecting production

Ice loads are divided in 7 classes and a power curve showing the median output power within each class is shown in Figure 4.4, together with its standard deviation. In general, the output decreases as the ice load increases. For all ice load classes, up to 13 m/s, the power output increases as wind speed increases. It should be noted that for the highest ice load, the turbine is standing still until the wind speed reaches 11m/s. It can be seen that the standard deviation is increasing with increasing wind speed for most ice classes. For ice loads [0.4 1) kg/m and [1 2) kg/m and wind speeds exceeding 14 m/s, both the output and standard deviation is decreasing to zero. Turbines at Aapua have troubles with production above 15m/s. This is related to mechanical problems and is addressed by the manufacturers and will be solved [Pers. comm. Göran Ronsten]. As the wind speed reaches above 15 m/s some ice load classes contain zero observations and

the curve simply ends. The standard deviation may not be a suitable measure for the variance since negative ice loads do not exist in reality.

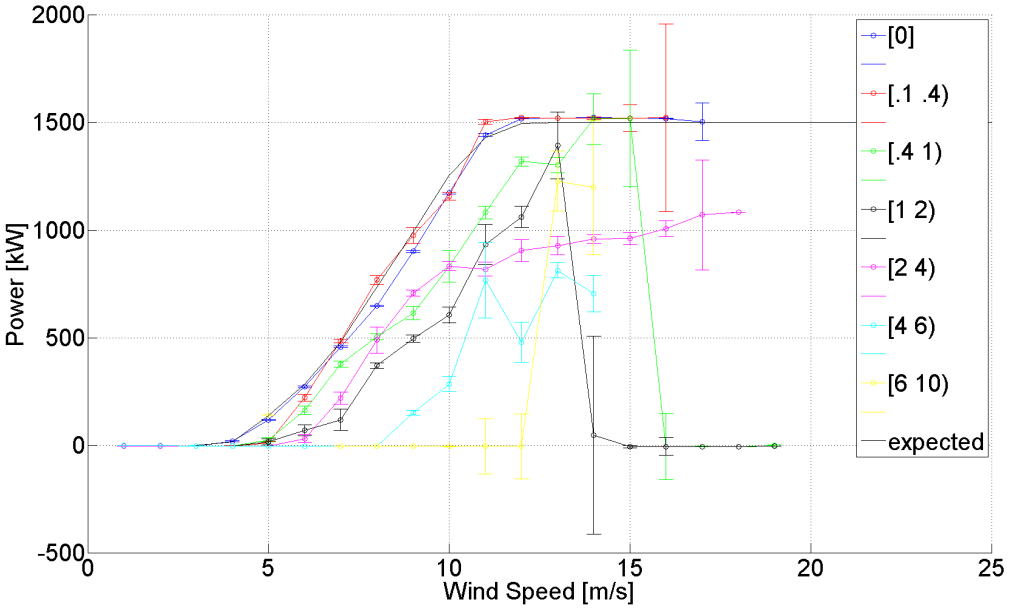

Figure 4.4: Median curves for each ice load interval using data from turbine 1. Errorbars give the standard deviation and ice loads are in kilograms [kg].

The relationship between ice load, wind speed and power output at Aapua is given in Figure 4.5, calculated using three different methods. The two first images are calculated from the boxgrid in Figure 3.3. The power output is shown as mean values at the top and median values in the middle image. The overall impression is that the median show higher power output than the mean. This is very clear where ice loads are high and also at high wind speeds for the lowest ice loads. For wind speeds above 16 m/s observations are sparse. In some cases the output is observed to be zero, and for winds speed above 18 m/s lack of observations give no result and therefore zero output. The last image is a weighted mean over the 50 nearest points, one grid point in Figure 3.4 representing each square in the image. The relationship show higher output values for high wind speeds compared to the "'box-method"' above. For ice loads above 6 kg and wind speeds between 10 and 14 m/s the weighted mean show a lower power output than the "'box-method"'.

Figure 4.6 show the standard deviation of the estimator from Figure 4.5. In general the median show a higher variance than the mean estimator and the weighted mean show the lowest standard deviation. In some cases like wind speed

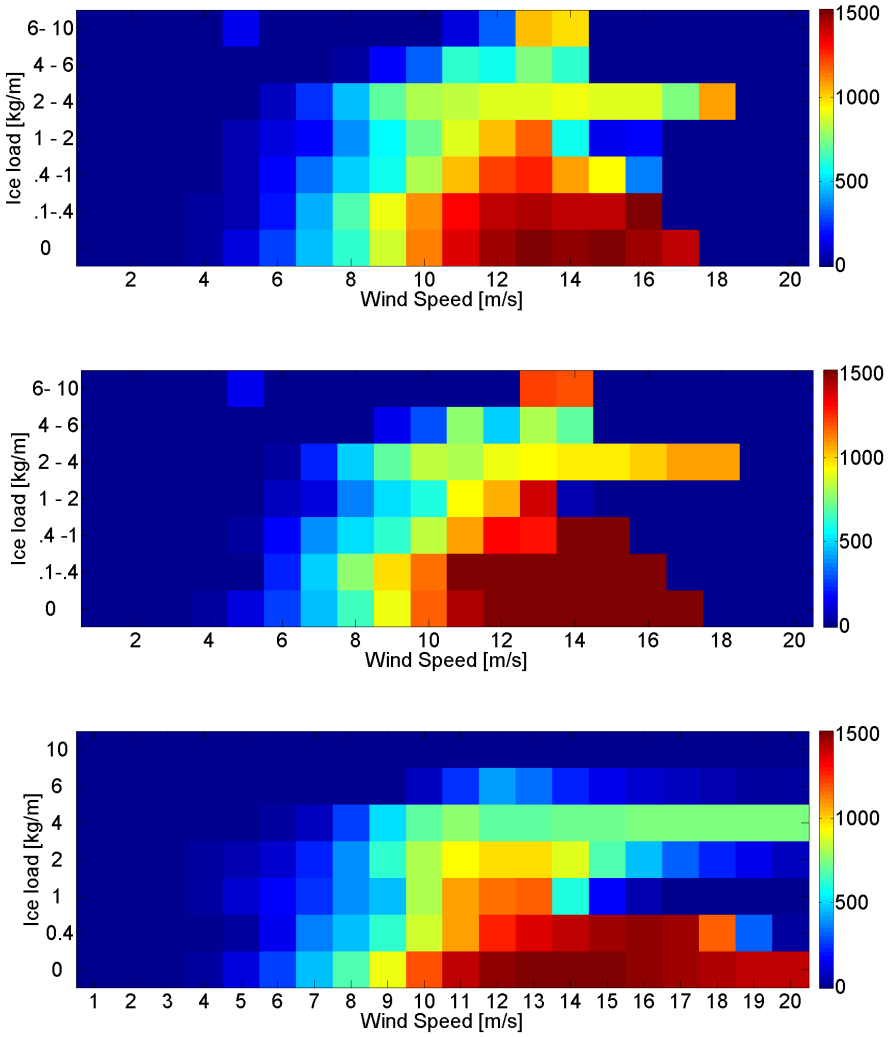

Figure 4.5: The mean (top), median (middle) and weighted mean (bottom) power output as a function of wind speed and ice load is shown in this figure. The colourbar indicates the strength of the power in kW. The top and middle image is based on the box-grid while the last is based on the 50 nearest observations around the chosen points in the kriging grid.

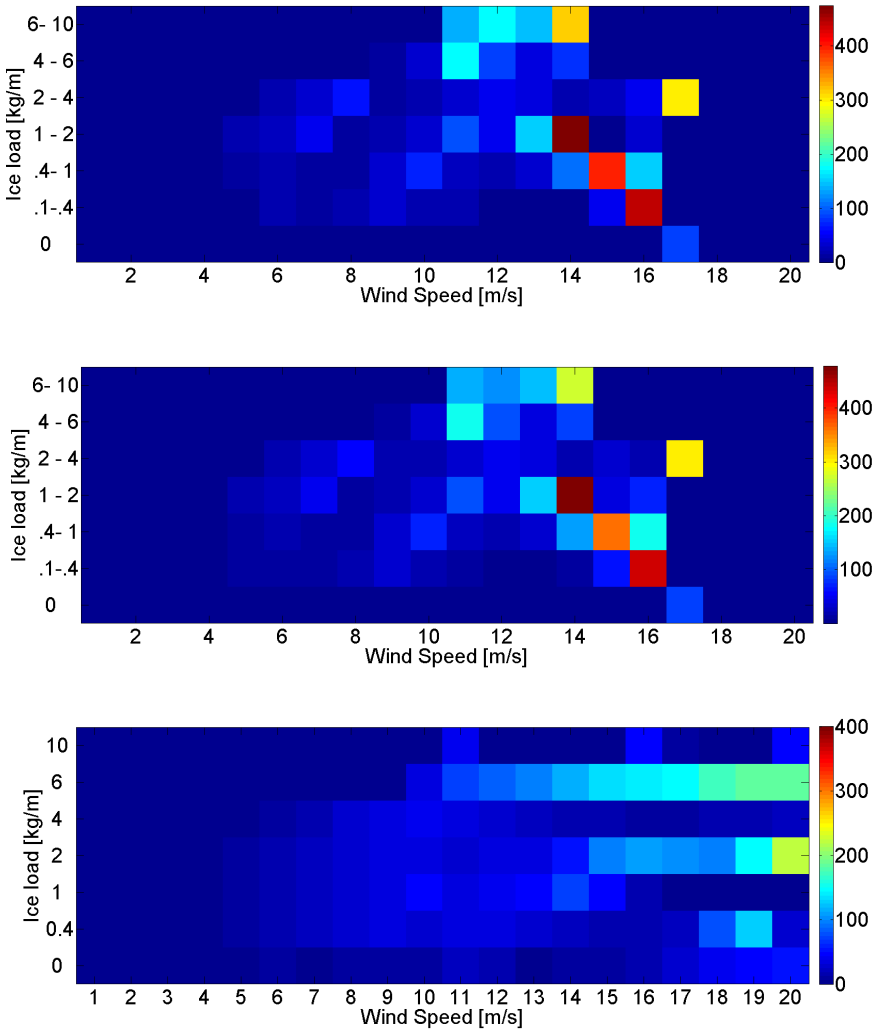

Figure 4.6: Standard deviation for the mean (top), and median (middle) using the box-method. Standard deviation for the weighted mean is shown in the bottom panel.

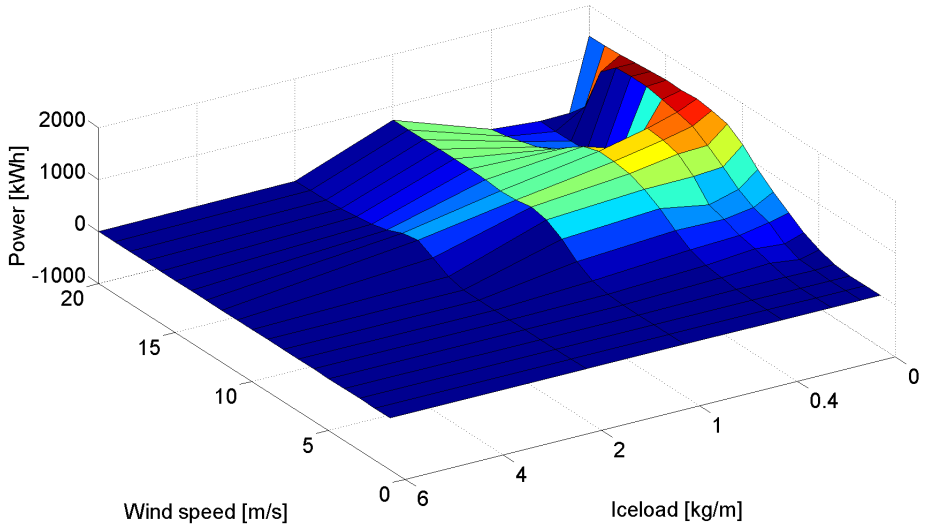

Figure 4.7: Output power as a function of wind speed and ice load is shown. The power curves are optimized for turbine 1, and is used as a model for the whole wind park.

from 10 to 12 m/s and ice load class 1, the mean do show a standard deviation while the median give zero. The overall tendency up to 16m/s is an increase in standard deviation for increasing wind speed and ice load. For wind speeds above 16 m/s observations are lacking and therefore the box-methods show no variance at all. The kriging method show results over the whole wind specter and the standard deviation are at times higher than what is observed using the box-method.

4.5 Model

The results obtained in kriging is shown in Figure 4.7. We may define this as a model though the function is not known. An optimized function will have to be based on more data. Interpolating linearly between grid points in Figure 3.4 give the surface and the output values outside grid points. It should be noted the lack of output for wind speeds above 15 m/s for all ice classes except around 0 and 4kg. Output is clearly decreasing for a given wind speed as ice is building on the turbine up to 15m/s. Above this level, output is dramatically decreasing before the model gives higher output for the ice load around 4kg. For ice loads close to zero the power output resembles the power curve for temperatures above 2^oC.

-	Observed [MWh]	$\hat{P}_{krig}$	Error	KVT	Error
October	7890	7134	-6.9%	8196	3.9%
November	6342	7125	12.3%	6497	2.4%
December	10098	8888	-12.0%	8588	-15.0%
January	5966	7413	24.4%	7506	25.8%
February	9769	9124	-6.6%	9283	-5.0%
March	15022	14882	-0.9%	11967	-20.3%
SUM	55088	54566	-0.9%	52037	-5.5%

Table 4.3: Key numbers for the measured and modeled production for the whole wind farm at Aapua. Observed output is calculated from the cleaned data and the model uses observed wind speed and ice load from the corresponding dates.

The performance of the kriging and KVT models for the whole wind farm at Aapua is shown in Table 4.3. The overall result for one year is good for the kriging model with an underestimated production of 1%. The KVT model shows an underestimating of 5.5%, compared to the observed result. The accuracy on shorter periods is significantly lower. In months where heavy icing is experienced, especially January, the loss is clearly underestimated by both models. March is a month of low loss, where little icing occurs and the result from the kriging model show only a deviation of 1%. The KVT model underestimates production with 20%.

Turbine	1	2	3	5	6	7	Total
Kriging	0,941	0,939	0,953	0,922	0,902	0,938	0,936
KVT	0,916	0,929	0,935	0,924	0,898	0,930	0,927
Box mean	0,207	0,188	0,251	0,184	0,076	0,172	0,182
Box median	0,206	0,181	0,240	0,172	0,077	0,166	0,176

Table 4.4: The correlation between measured and modeled output for kriging, KVT and Box models.

Table 4.4 shows correlation between modelled and measured observations for cleaned data. The kriging method show the best result for all turbines. Turbine 1 which is used to make the model do not show any significant difference in correlation compared to other turbines. The KVT model show a lower correlation than the kriging model, though the result is significantly better than for box-methods.

The root mean square error (RMSE) for all models can be seen in Table 4.5. The RMSE is significantly lower for the kriging and KVT models. The kriged model show the overall best result. The KVT model show a higher RMSE for all turbines and the RMSE for box-models are significantly higher.

Turbine	1	2	3	5	6	7	Total
Kriging	170	170	142	198	233	185	175
KVT	205	188	176	195	251	209	194
Box mean	603	591	549	614	610	627	590
Box median	607	595	553	618	613	630	593

Table 4.5: The root mean square error (RMSE) for four different; KVT, Kriging, box mean and box median.

4.6 Evaluation of model

Kriging is considered the most robust model and an evaluation of its performance is done. Data from turbine 2 is used to evaluate the model during all of the next examples. The "'no ice"' power curve is the pure power curve as it is when there is no ice on the blades. In all plots, the wind speed can be partly estimated from the "'no ice"' curve since wind speed is the only input. Small variations within the highest wind speeds are not easy to distinguish due to the fact that the turbine should produce maximum from 13 m/s.

Figure 4.8 show measured (blue), modeled (red) and "'no ice"' (black) power output during a period in March where the model fits well with the measured production. The expected output calculated from only wind speed, show the same values as the modeled and measured power which means the ice load is sparse or non-existing in this period. The ice load can be seen in the bottom image of the figure. The variance in ice load is most likely noise during this period. It should however be noted the abrupt increase in ice load on March 15th and the decrease on the 16th where a negative ice load of 0.2 kg is measured.

Figure 4.9 show measured (blue), modelled (red) and "'no ice"' (black) power output from January 15th to 21st on the top panel and the measured ice load on the bottom panel. It can be seen how modelled output varies as the ice load changes. As soon as icing is recorded on the cylinder, the reaction in power output is registered late January 15th. The model underestimates the loss in the beginning of the event. The modelled and measured output then follows each other after the icing has lasted for one night. This continues for several hours until an increase in ice load is registered early 16th. Then as ice load exceeds 1 kg the model again underestimates the loss. From late January 16th to January 19th, the ice load stabilizes and the modelled output follows the dynamics of the "'no ice"' curve, only shifted due to the ice load. The measured power however, is changing significantly during the same period. Late January 16th and early January 17th, the modelled output is overestimated compared to measured power. As the ice load is stabilizing and decreasing slightly, the measured power catches up with

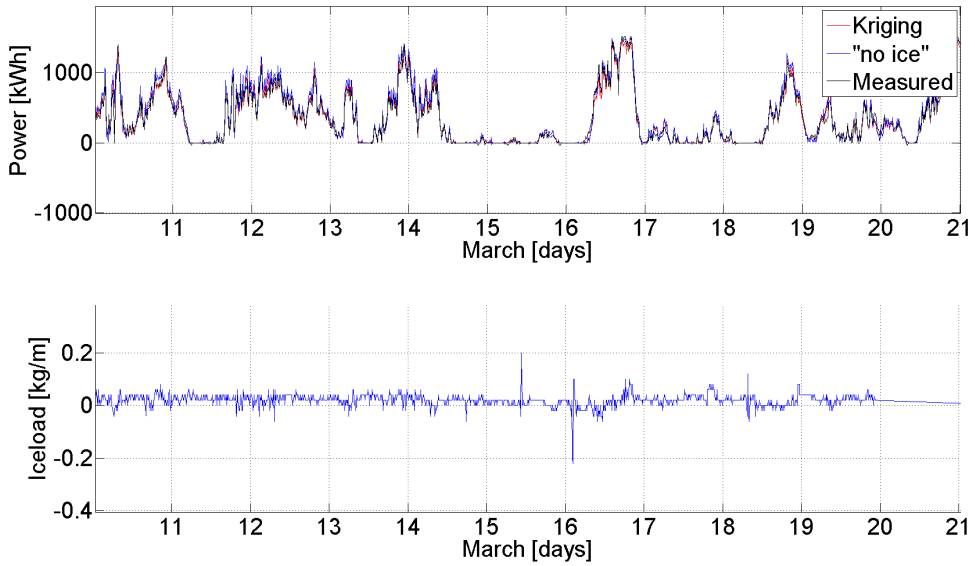

Figure 4.8: Measured, modeled and expected output in March in the top image. Ice load during the same period is shown in the bottom image.

the modelled power midday January 17th. The measured power then increases and through the next day show higher output than the model.

The measured (blue), modelled (red) and "'no ice"' (black) power output from January 18th to 20th is shown in the top panel of Figure 4.10. The bottom panel show the measured ice load and temperature during the same period. It can be seen that the modelled power output is underestimated on January 18th. On January 19th and 20th, the modelled output follows the curve of the measured output quite well. The ice load during this event is changing from 1 to 2.5 kg/m.

Figure 4.11 shows a period where the model is in general overestimating production compared to the measured result. In this figure heavy icing occurs in most of the period. Late January there is a total buildup of 10 kg of ice on the cylinder which abruptly falls off. The modelled output increases immediately to a higher level while the observed output continues to give zero output. The turbine has been stopped in parts of this event but observations exist which means the turbine is not stopped the whole time. It should be noted the modelled output during January 27 which is very low at one point during high wind speeds.

In the November results, shown in Figure 4.12, it is easy to identify a clear mismatch between the ice sensor and the turbines. During November 10th and 11th

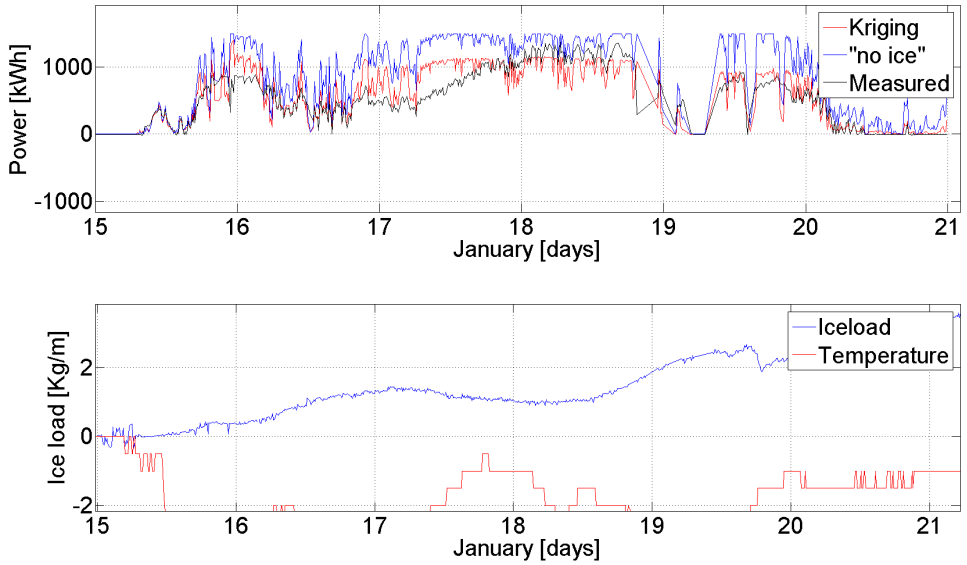

Figure 4.9: modelled, measured and "'no ice"' output from January 15th to January 21st in the top panel. Bottom panel shows temperature and ice load.

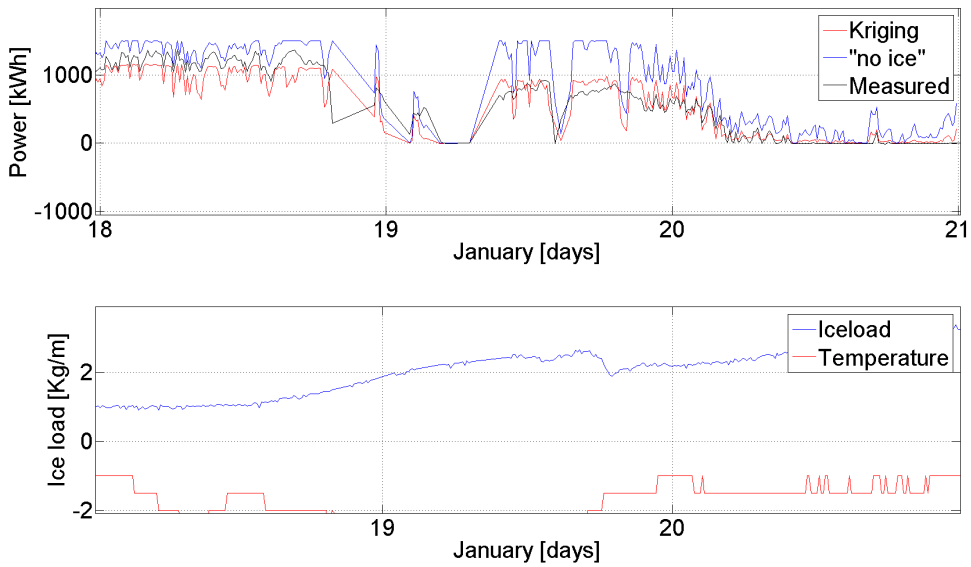

Figure 4.10: Measured, modelled and "no ice" power output is shown in the top panel

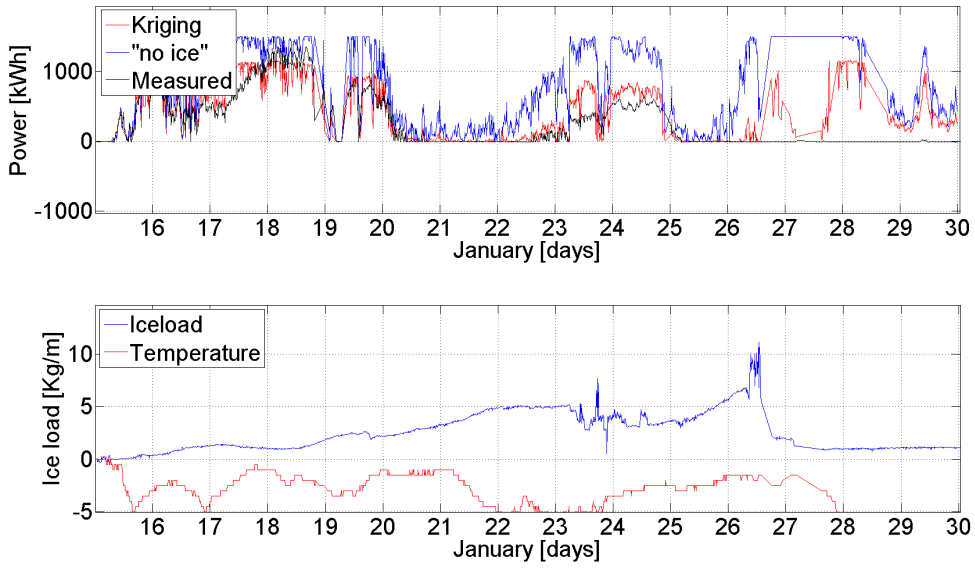

Figure 4.11: Top panel show measured, modelled and "'no ice"' power output from January 15th to 30th. Ice load for the same period is shown in the bottom panel

the model follows the production very well until a sudden increase in modelled output at noon the 11th. The ice sensor has not measured the exact fall-off, but due to measurements just before and just after, the event is captured. The modelled production increases immediately due to the decrease in ice load. In the following days the model shows an overestimated production. The sudden ice-fall happens while temperatures are below 0^0C therefore it is not likely that melting has occurred.

Figure 4.13 show how the model underestimates the production on November 15th to 16th. The model is following the measured output until late evening 15th. As the temperature increases above 0^0C, the measured output increases. The wind speed is stable, and relatively high at the time, judging from the "no ice" output. During this event, the turbine gain effect faster than the model which show a low output until the sudden fall-off of ice on the 16th. At the end of this period the model follows the production again.

The presented examples were chosen among many, and should resemble the overall impression of the performance of the model and also explain the relationship between ice and power production as it is measured and observed at Aapua.

Variance is thought to decrease if more observations are used to calculate the

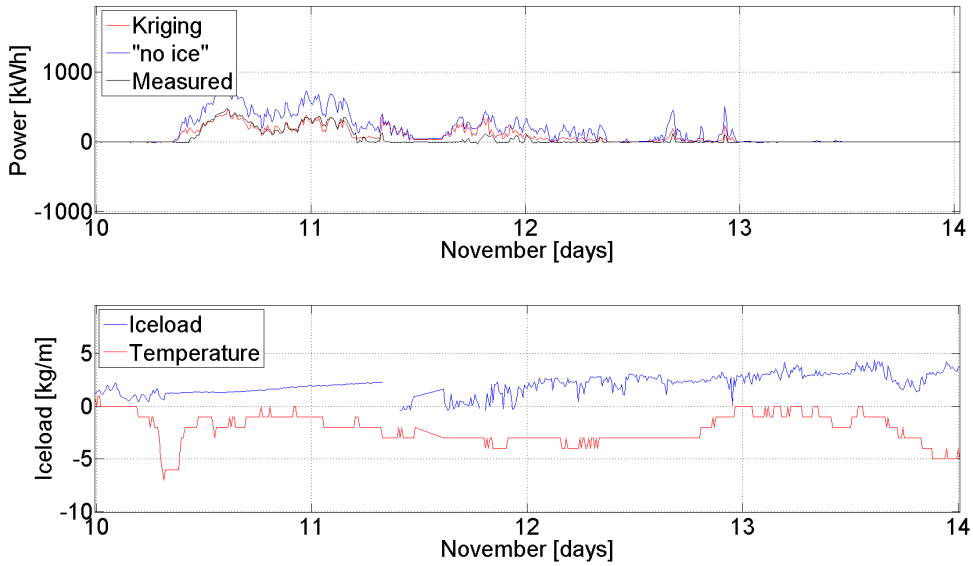

Figure 4.12: Measured, modelled and "no ice" output from November 10th to 14th is shown in the top image, the bottom image give the ice load during the same period.

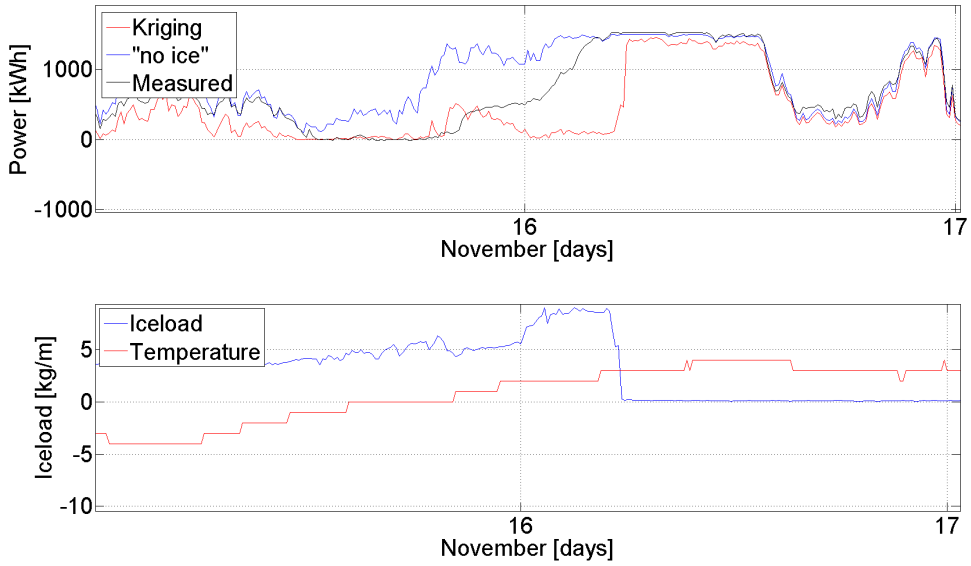

Figure 4.13: Measured, modelled and "no ice" output from November 14th to 18th is shown in the top image, the bottom image give the ice load during the same period.

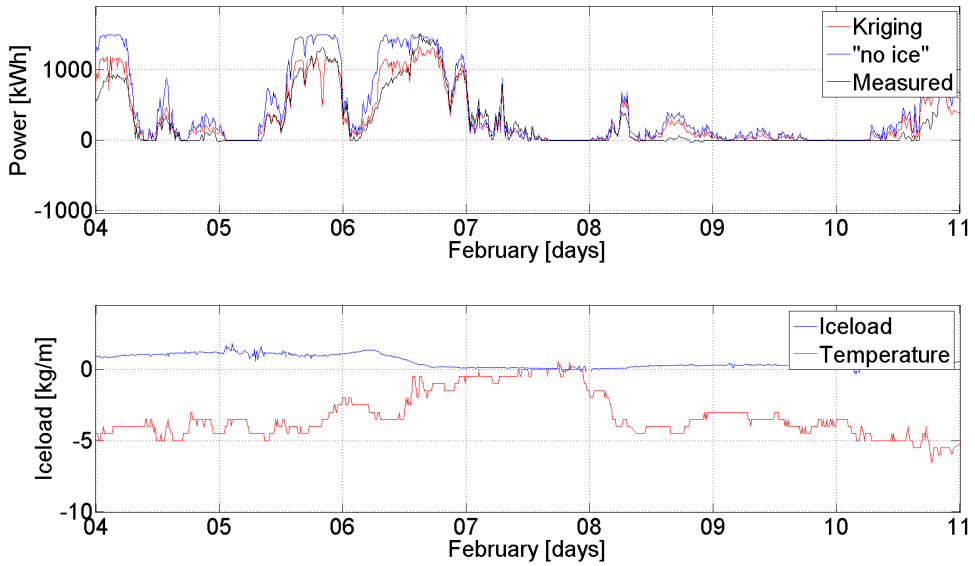

Figure 4.14: modelled, measured and "no ice" production for February at the top. Ice load and temperature during February at the bottom.

models power curves. Data from all turbines could be used to improve the model in this paper. However this is not done here and is a suggestion for further development. Other data should then be provided to test the model.

4.6.1 Sublimation

Analysis shows that there are events where ice on the measuring stick disappears during periods of cold weather. No melting is observed during these periods. In the morning on February 6th the load on the measuring cylinder show 1.5 kg/m, Temperatures are recorded below zero during the actual time. Late February 6th the ice load has decreased to 0 kg/m. Figure 4.14 show a plot of the temperature, ice load and response in production during the event. There is a relatively high wind speed during the day and humidity is dropping from 85 to 65.

4.7 Events correlated in time

A plot of all observations containing wind speeds between 8.5 and 9.5 m/s within an ice load of 1 and 2 kg is shown in Figure 4.15. The grid lines mark the events where there is a gap of more than 24 hours between the measured observations.

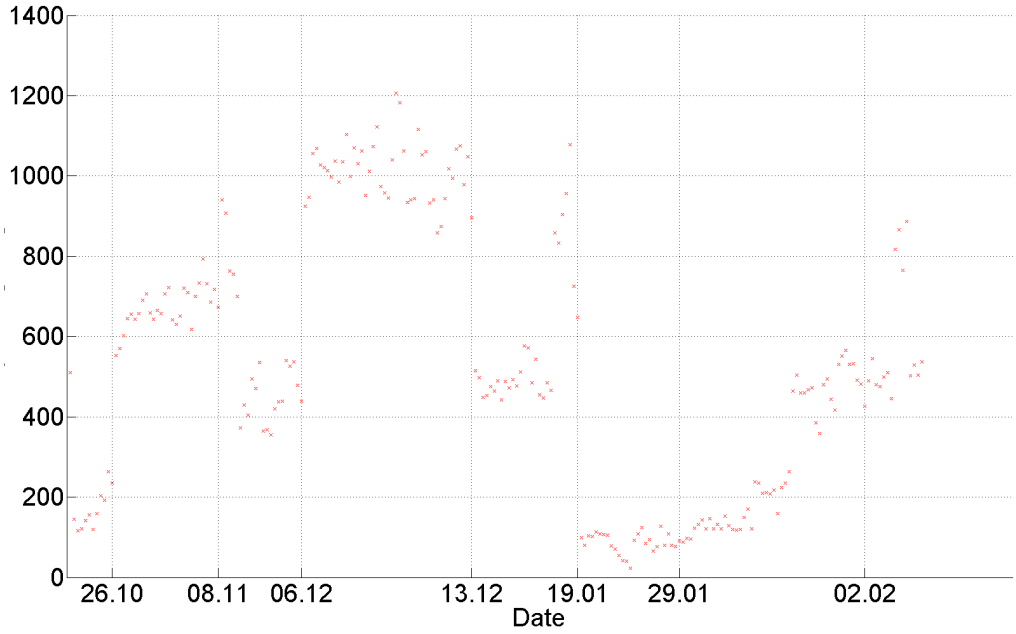

Figure 4.15: Plot showing all measurements within the ice class from [1 2) kg/m and wind speed ranging from 8.5 to 9.5 m/s. The grid lines are labeled with a date which shows the sample date in the event up to the grid line.

The point exactly on the grid, show the last observation in the clustered sequence. Figure 4.15 shows large variance within the specific box of wind speed and ice load. The main interest in the plot is that power output for each event differs significantly; an output in power from zero to more than 1200 kW is observed. Samples clustered in time show a somewhat similar power output, if there is observed a long time gap between the samples, there is a tendency that power output is changing significantly. The last measurement during January 19th, gave an output of 700 kW. The next measurement, with similar wind and ice conditions, is at least 24 hours later and show an output of only 100 kW. The "no ice" output $\hat{P}(V)$ considering only wind speed is from approximately 850kW to 1100kW. The modelled output $\hat{P}(V, I)$ is between 500kW and 750 kW.

4.7.1 Weekly analysis

The power output and ice loads are summed up for every week during the season. The result show that the largest contribution to production losses are given during short time intervals. The last week of January, where icing is significant, the loss reaches more than 85%. Also November and February has a period of severe icing

where losses reach 55%. There are weeks during the same months where there is no loss at all.

During the last week of December in 2009 and the first week of January in 2010 the meteorological measurements where not recorded and therefore there are only ice load measurements available from these two weeks.

October	Observed[MWh]	"No ice"	Loss [%]	ice [kg/m]
[1 7]	299	390	23,5 %	118
[8 14]	559	586	4,5 %	145
[15 21]	622	680	8,5 %	187
[22 31]	76	145	47,9 %	1541
November				
[1 7]	447	493	9,3 %	216
[8 14]	77	174	55,6 %	1521
[15 21]	205	381	46,3 %	1007
[22 31]	425	698	39,1 %	212
December				
[1 7]	529	612	13,6 %	561
[8 14]	404	413	2,1 %	741
[15 21]	579	569	-1,7 %	125
[22 31]	0	0	NaN%	84
January				
[1 7]	0	0	NaN%	93
[8 14]	309	309	0,0 %	36
[15 21]	427	681	37,3 %	1042
[22 31]	108	781	86,2 %	3412
February				
[1 7]	241	535	54,9 %	899
[8 14]	300	373	19,5 %	212
[15 21]	218	211	-3,2 %	88
[22 31]	348	364	4,6 %	6
March				
[1 7]	522	548	4,9 %	13
[8 14]	472	506	6,7 %	19
[15 21]	258	274	5,7 %	14
[22 31]	608	631	3,7 %	18

Table 4.6: Production and production loss per week.

Chapter 5

Discussion

5.1 Cleaning data and distribution of observations.

Cleaning of data eliminates all observations done when an alarm code is triggered. This will most likely eliminate some observations where icing is the reason for the alarm. Frozen instruments or increased maintenance work, which stop or alter the turbines performance, should result in an alarm code being triggered. The loss in these cases could be due to icing, but this is not detected by the method used in this thesis. Instead, production loss due to icing will mainly be losses while the turbines are actually working.

Cleaning data the way it is done here, may therefore underestimate the total production loss due to icing. To estimate the total effect of icing, alarm codes should be investigated and the observations included correctly so that "ice triggered" alarms are calculated within the loss. On the other hand, if no cleaning was done, several cases of wrong wind measurements would lead to more recorded overproduction and therefore lower loss. Also stops due to normal routine maintenance work or instrument failure, power stops etc which has nothing to do with icing would increase the calculated loss. However, the applied method for calculating the power loss is supported by farm owners [G. Ronsten, pers. comm.].

From the distribution of observations, there are observed cases of high winds where production is zero, as seen in Figure 4.3. Since these events occur in the cleaned data, the reason is thought to be heavy icing on the turbine wings itself, simply preventing the airflow to start the rotation of the rotors. It could be that turbines are manually stopped during the heaviest icing events. All stops, including manual stops should, as mentioned, trigger an alarm code. The observations shown in Figure 4.3 are therefore most likely not due to manual stops.

A $+2^0C$ power curve calculated from actual production numbers is used to define expected output, as explained in 3.2. The median during the rest of the season can be shown not to deviate significantly from this result unless icing or other effects occur. It can be argued that overproduction is not detected as a single parameter using this method. An increased overproduction could be expected through December, January and February due to the higher air density in cold periods. If so, the loss due to ice can be underestimated. This since the difference between expected power and measured power could give a negative loss when the measured power is larger than the $+2^0C$ power curve. In any case the losses due to icing will not be overestimated.

Observations done where overproduction is unrealistic high, are eliminated. High production during low winds give a very high measured production compared to what is expected. If not filtered, these observations could make the loss due to icing significantly underestimated. The fact that the filtered observations are clustered in time, as shown in Figure 4.2, is consistent with frozen or broken anemometers. If they were spread randomly, the high output on small wind speeds could have other unidentified reasons. Two measurements done during the time of the filtered observations, were not filtered out. According to their observation date they should have been filtered, but due to their output being just within the limit of what is considered possible, they are calculated as part of the cleaned data. Samples like this may, and most likely will, occur and could only have been avoided if every single sample was investigated. Another approach to the issue could be to define a maximum deviation from the $+2^0C$ power curve and define deviation from this as overproduction and loss, depending on which way the deviation goes. This method was used by [Homola et al., 2009], however, this method most likely underestimated the total loss. The anemometers are heated and should work under icing conditions, though heavy icing may cause the measured wind speed to be lower than actual wind speed as seen here.

5.2 Total production and loss

The total production during the winter 2009-2010 calculated from cleaned data give a loss of 16.000 MW, or 25%, for the wind farm as a whole. The highest loss is found in January, which alone stands for a loss of 7.000 MW, or 52% of the expected production during this month. The monthly loss during the whole season varies from 52% in January to only 0.9% in March. Using turbine 2 as an example, Table 4.6 show that one week in January experienced a loss of more than 80%, indicating that severe production losses are concentrated in time. In Figure 4.3 it is seen that the observations are mainly clustered around the power curve. This means the turbine is operating normally, and producing the expected power

output, most of the time. The observations causing loss in production are low in numbers, which indicates that the majority of production loss comes within short periods of time. This correlates well with the observed loss during one week in January.

The most severe losses for the wind park as a whole are concentrated to the months where the largest amounts of ice are registered. The few weeks with heavy icing and high loss for turbine 2 in November, late January and early February seen in the weekly analysis is an indication of the same. This means that the highest ice loads most likely gives the most severe loss. If events like this are recognized it might be possible to avoid the worst effects. A turbine standing still for several days during high winds causes a huge loss. After detecting the event, action might be taken to avoid the loss to last for several days. As prediction of ice is improving [Øyvind Byrkjedal and Berge, 2009, Nygaard, 2009], production losses can probably be further decreased since action can be taken earlier.

5.3 Ice affecting production

That ice is affecting production has been shown using production numbers during the winter season, as seen in Table 4.1. How the different ice loads influence on turbine performance according to the observations is visualized in Figure 4.4 with median curves. It is obvious that as ice accumulates, the performance of the turbines are lowered. This is consistent with the work of for example [Seifert and Richert, 1998, Barber et al., 2009, Virk et al., 2010]. With wind speed from 3 m/s to 13 m/s, a decrease in performance for increased ice loads is easy to identify. As the wind speed increases above this level the response in power output is not following the same pattern. Ice loads up to 0.4 kg/m continues to give maximum output, though the standard deviation is increasing above 15 m/s. Power curves for ice loads between 0.4 kg/m and 2 kg/m, drops suddenly to zero above 13 m/s, while the 2-4 kg/m continues it's slow increase as wind speed increases. Reasons for the different responses are discussed further under Section 5.4. Power output for the two highest ice classes is only observed up to 14 m/s, and the curves end here.

In general, for wind speeds up to 13m/s, the power curves resembles the power curves produced by [Seifert and Richert, 1998], which can be seen in Figure 2.12. Seifert show how rotors experiencing ice covering a small part, 3-6% of the blade, are affected during low wind speeds. Still, the turbine will reach rated power, only at a higher wind speed than if no ice was present. As the ice cover increase, the turbine will never reach rated power but flatten its production before maximum output is obtained.

The theoretical model, KVT, is thought to perform well for the mentioned events since it is based on Seifert's idea. Above 15m/s the observed power curves from Aapua differ more from the theoretical by giving zero output were Seiferts results give output. It should also be mentioned that the ice covering the blades made by Seifert differs in quality and shape, which also influence the effect on performance, as shown in Figure 2.12. Ice load, as it is measured on Aapua, could resemble the ice covering of the blades as Seifert shows by assuming that the higher load measured, the more of the blade is covered. However, the accreted ice on the cylinder and turbine blades at Aapua may also differ significantly in shape and quality, though no measurements are available to investigate it in this thesis.

5.4 Modeling methods

Three different statistical models, $\hat{P}(V, I)$, based on observation data from turbine 1, are presented in Figure 4.5. The box-method is shown in the top and middle panel, and the models output are calculated using mean and median values, respectively. The box-method show exactly how output will be calculated for every input of wind speed and ice load (V,I). Both mean and median, will produce results at all locations where observations exist. If observation data from turbine 1 do not exist, a zero output is produced, see for example wind speed 18 m/s and 0 kg/m ice load. When the model is tested on turbine 2, with input within the mentioned box, the calculated output will be zero. Lack of observation data at this wind speed and ice load, when producing the model, cause the zero output. This is a disadvantage with the box-method. The method is also found to be doubtful in cases were only one measurement is found within a specific wind speed and ice load box. This can be observed when investigating the standard deviation for the estimator in Figure 4.6, and the spread of observation data within the boxes in Figure 3.3. Standard deviation increases as the number of observations decrease, until data within one box consist of a single observation. Then the standard deviation goes to zero. Thus the method should be used only when the number of observations is sufficient to produce output for the whole wind and ice specter.

Both box-models show an increase in output for 13-14 m/s as ice load increases from [4-6) kg/m to [6-10) kg/m, which is very unlikely. Power output is thought to decrease with higher ice load. Since models are based on empirical data, a closer investigation of the happenings around 6-10 kg/m of ice may explain the high output. The reason can also be sparse observations where outlayers will have large influence on the output. The median was used to avoid the influence of outlayers, but here the number of observations is so few that the median still gives a high power output. In cases were few observations are available, the wrong measurements have a greater influence. The standard deviation in these cases are

also very high, which indicates a large internal deviation between measurements within the boxes. This supports using another method, especially for sparse observation data.

As kriging is applied, the calculated production during the highest ice load is significantly decreased and output for 6 kg/m of ice is also decreasing. Based on theoretical studies, e.g. [Jasinski et al., 1998], the kriging results seem realistic, especially up to 15 m/s in wind speed. Power production at lower wind speeds and lower ice classes are roughly the same using either the kriging or the box methods, and these results are close to the theoretical ones. The numbers of observations are significantly higher in this part of the ice and wind range, which leads to estimates with low variance. The standard deviation is also lower for these cases. This indicates that a sufficient number of observations is needed to obtain a reliable result for both methods; the more observations, the better reliability. Since standard deviation using kriging is generally lower, compared to the box-method, kriging could perform better here. Kriging should, according to theory, perform better where data is sparse. However, it is observed higher standard deviation for the weighted mean in kriging compared to the box-method at locations of high wind speed. This can be explained by the fact that no observations are originally found here. The box-method calculates zero variance due to zero observations. The kriging method provides result at unobserved locations by estimating the value from nearby location. Thus, an increase in standard deviation is simply due to the fact that more samples are used in the kriging estimate. The higher output for ice loads around 4 kg/m is illustrating this; According to Figure 3.3 no observations from turbine 1 are found at 4 kg/m of ice and wind above 15 m/s. The power output is thus estimated from the output at lower wind speeds. The same 50 points then provide the values for several locations and therefore show identical results for all higher wind speeds.

Reasons for the low output values around ice loads of 1 kg/m and wind speeds above 15 m/s have been discussed. Investigating the raw data, from which the model in this region is based on, tells us that observations exist during ice load around both 1 kg/m and 2 kg/m up to 19 m/s, see Figure 3.3. The model output resembles the power observed in the data closest to the grid point. Observations done during the highest wind speed show an ice load of 1-2 kg/m from Figure 3.3 and zero in output from Figure 4.3. The model is therefore resembling exactly what is observed on turbine 1; no output for 1 kg/m of ice at wind speeds between 15-19 m/s. Testing the model on data from turbine 2 is thought to explain the reason for the low output at apparently high wind speed as interpreted in the following.

In January the highest winds, up to 19 m/s, are observed also for turbine 2. During the last week of the month, ice accumulates on the cylinder and also on

turbine blades according to the lowered performance, see Figure 4.11 The load exceeds 6 kg/m and the turbine does not produce any power, probably due to the heavy icing. During temperatures below zero and high wind, the ice is suddenly disappearing from the measuring cylinder. The weight drops dramatically from 10 kg/m to 2 kg/m during an extremely short period on January 27.

A possible explanation to the abrupt fall-off from the cylinder could be instrument failure. If ice accumulates and bridges over to the foundation, the rotation of the instrument will stop and an ice flag will build against the wind. With an increase in temperature, heat from the instrument in addition to wind may cause the ice to fall off abruptly. The temperature is low at the time which means the wind will have to be the main reason for the fall-off. It is at least not induced by melting according to the temperature measurements. At the same time the ice on the turbine blades is probably not falling off. Zero output is measured for several days until February 2nd. Then a small amount of power is produced before again the turbine stands still. The zero output in the model can thus be explained by the mismatch between cylinder measurements and actual load on the turbine.

Since output is interpolated between grid points, all nearby wind speeds and ice loads are affected by the mismatch, creating a valley of low output in the model for 1 kg/m of ice and winds between 15-20 m/s. If the ice building and shedding on the cylinder were more correlated to the actual ice load on the turbine blades, the model output should improve significantly. Also, elimination of the actual observations, or simply putting the ice load to 10 kg/m, during the period from the ice falls off to the turbine starts producing again, could reduce the problematic ice readings in this particular event. In any case, more observations during high wind speeds should improve the result.

5.5 Testing models

When the box-method is applied on observation data, taking wind speed and ice load, (V,I), as input, the output, $\hat{P}$ will be the same for all inputs falling within the same box. For kriging, the output value is estimated according to the position (V,I) in the grid. If (V,I) is not exactly on a gridpoint, the linear interpolation between grid points will give the resulting power output. For example during wind speed 12 m/s, an ice load of 2.0 kg/m will give the same production, 900kW, as an ice load of 3.9 kg/m. The kriging model in comparison will, for the same wind speed, give 1000kW for 2 kg/m of ice and 700kW for 3.9 kg/m. The RMSE calculated for all methods using data from turbine 2, show a very high RMSE for the box-methods. This is probably much due to what is explained above. A suggestion for an improvement of the box-method could be to let the value,

which is now representing a whole box, only represent the middle point of the box. Then, interpolating linearly between the middle points of all boxes would give a unique value for every input (V,I). This resembles more the approach of the kriging method and can thus reduce the RMSE. According to the RMSE, which is lower for kriging, the kriging model resembles better the measured power output. The RMSE for the KVT model is, as for kriging, quite good, though the kriging model show the best result.

The correlation is also significantly lower for the box-methods. The dynamic of the data using the box-method, will not be detected very well since several different inputs(V,I), will produce the same output $\hat{P}$. Whereas the kriging method will resemble the dynamics by giving different outputs for every input. The latter is also the case for the KVT model. Based on correlation and RMSE, the kriging and KVT model is found to perform significantly better than both box-models. The best correlation is shown to be the kriging model, but the KVT model also performs quite good.

Looking at the overall result for the kriging model in Table 4.3, it is seen that the modelled output for the winter season as a whole only deviates 0.9% from the observed value. The KVT model gives a larger error and is overestimating the production with 5.5%. From the same table, the kriging model is observed to perform best in cases with low ice load. March is a month with almost no ice accumulation and the kriging model shows a deviation of only 0.9% from modeled to measured power. The KVT model show a significantly higher error for March with underestimated production of 20%. This may be due to the KVT model having a maximum value of 1500kW while the kriging model is based on the actual output from Aapua which can sometimes be higher. During January, which is the month with the heaviest icing, none of the models performe satisfactory, and the kriging model shows the best result, overestimating production with 24%. In desember the the kriging model underestimates the production with 12% whereas in November, production is overestimated with 12%. The deviation between the two months is large and a further invastigation of the short term events is needed to explain the reasons. The KVT model also show a large deviation of modeled output for the two months, with 2.4% overestimation in November and underestimating production with 15% in December. The error in estimated power output is significantly increasing for monthly output compared to the whole year.

Time series using the kriging model with input from turbine 2 is investigated and analyzed to find reasons for the mismatch on short terms and its failure during heavy icing events. From Figure 4.9 it can be seen that as ice starts accumulating late 15th and early 16th, the model overestimates the production. Then the ice load stabilizes and the measured output "catches up" with the model. The modeled and measured output then follow each other for a short period until the

ice again starts building late 16th. Then the model is again overestimating power production. As the conditions stabilizes on the 17th, the model gives an output which is stable in times of following the "'no ice"' curve, only shifted due to the ice load. The measured output however, is increasing significantly during the stable conditions on the 17th. Late the same day the measured power has increased beyond the modeled, which now underestimates the production. Every time the ice starts building on the cylinder, the model overestimates the production. This indicates that icing is most severe for the performance of the turbine during accumulation. According to collision efficiency, the tip of the blade will have the ability to hit a significant amount of droplets compared to a measuring cylinder only rotating around its own axis. Accumulation is therefore most likely faster on the turbine than on the cylinder. This can underestimate the ice load on the blades, especially while accretion is ongoing.

The icing rate, measured by the Holo Optics, could be used to investigate this further. The icing rate could confirm if accretion occurs during all periods where turbines are producing less power than modeled due to ice load. Increase in weight on the cylinder will also indicate accretion. Since the results from the cylinder has shown to not always resemble what is happening on the turbine blades, the ice rate sensor could give a more reliable result. Unfortunately, time did not allow for a closer investigation of the icing rate in this thesis. Instead, this could be a topic for further research.

An example of how the model and measured output reacts on melting processes is shown from November 15th-17th in Figure 4.13. Modeled and observed production follow each other during the 15th until production is underestimated by the model from late November 15th to midday 16th. The impression is here that ice accumulates on both the blades and the cylinder; this is confirmed both by the ice load weight and the lowered performance of the turbine. Then, as the temperature is rising to $+1^0C$, the ice shed from the rotors significantly faster then what is the case for the cylinder. The model clearly underestimates the production at this point, which again contributes to the need of an ice measure which better resembles the real ice accumulation and load on the blades. The rotational speed of the turbine blades will increase the chance of shedding compared to the cylinder, and thus increase the mismatch between ice loads on the two structures.

An opposite situation is also recorded during the same month, see Figure 4.12. Around noon, November 11th, ice is falling off the cylinder during a period with cold temperatures. The event is considered too fast to be due to a normal sublimation process. The increase in modeled output is recognized immediately as ice falls from the cylinder, resulting in an overestimation of power output. In this case ice is probably still present on the blades of the turbine while the cylinder holds no ice. A suggested reason for abrupt fall-off of ice has been discussed ear-

lier under 5.4. This shows that the model is built on the cylinder measurements, which can not fully represent the actual ice conditions on the turbine blades.

Sublimation is another process that complicates the modeling based on ice load. The event explained in Figure 4.14 show how ice load is decreasing during cold temperatures. This is most likely not ice that falls off, since the change in ice load is slow and smooth compared to the January 27th event. Sublimation will occur as relative humidity is decreasing so that ice can evaporate without melting first. This process is controlled by air humidity and exchange of air around the sublimating ice. On February 6th, a sublimation process occur on the cylinder. The measured output increases faster than the modeled during the day and afternoon. Half way in the sublimation process the measured power has increased to a higher level than the modeled. Since turbine blades are rotating at a faster speed then the measuring cylinder, the exchange of air is faster, thus allowing more ice to sublimate. Due to the slower sublimation on the cylinder, this event results in the model being "'to slow"' to catch the process that is actually happening on the rotors.

As the measurements on the cylinder is not always well correlated with what is happening on the turbines, a closer look at the variation within one ice load and wind speed class is shown in Figure 4.15. The large variation presented here can be explained by one, or a combination of the following factors: Ice fall-off (malfunctioning ice monitor) and sublimation, melting and accretion processes which behave differently on the cylinder and the turbine blades. Different types or quality of ice could also interfere and introduce variability in the measurements. Glaze, rime and wet snow all have different characteristics and different effect on a turbine regardless of weight [Seifert and Richert, 1998]. By plotting the power output within a specific wind speed and ice load, the variety of turbine performance can be detected. A closer examination of this plot shows that as an event is started it is highly possible that the power output pattern is similar as long as the icing condition is constant, as explained from Figure 4.15. This result may be used as input for a weather forecasting model in prediction of ice. A problem when estimating ice is to catch the correct load, though dynamics of the process is often found. By knowing the power production and icing in former hours, it might be possible to obtain a better short time prediction of icing and power production.

Chapter 6

Conclusion

Calculations of production losses has been performed on data from Aapua wind park during the winter season 2009-2010. After cleaning data, production loss at Aapua due to icing is calculated to 25% for the whole season. The total loss, calculated from raw data, results in 30%. The loss due to icing is probably underestimated, much due to filtering of all alarm codes in the cleaned data.

The highest loss due to icing is found during heavy icing events. These are found to be isolated events that are time limited. The longest event during the winter season in this study, was found in the end of January and consist of 21 consecutive days, starting on January 16th.

Two different methods, the "'box-method"', using mean and median, and kriging with weighted mean are proposed to estimate the power output model $\hat{P}(V, I)$. The model estimates power output based on wind speed and ice load observations.

Kriging shows to be better than box-methods based on standard deviation. Kriging also gives output for the whole specter of wind speed, while box-methods give zero output where observation data did not exist when the models were made.

Comparing all models, including KVT, the kriging model is found to perform best based on correlation and RMSE with data from the whole season 2009-2010. The mean and median box-method gives a very low correlation and high RMSE. The difference between the kriging and KVT model however, is smaller. The kriging model gives a lower error in modeled power output, decreasing the RMSE from 194kW to 175kW. The main difference between these models is estimated power output during times of low ice loads, where KVT underestimates production with 20% in March, compared to 1% for the kriging model.

The kriging model performs well for low wind speeds and low ice loads. During

times of heavy icing the model performance is not that good, with an overestimation in power production of 24% during January. The available empirical data are found insufficient in numbers to produce a statistically reliable result. One reason for this is that the turbines at Aapua have problems with producing above 15 m/s, which leads to large variation and dubiously power estimations above this wind speed. A sufficient number of observations is critical in obtaining trustworthy results for the power model.

The mismatch between what is happening on the rotors compared to the cylinder is causing large differences between real ice load on the turbine blade and measured ice load. Malfunctioning of the ice monitor during heavy icing events leads to larger errors, e.g. when ice suddenly disappears.

In addition, with a fully working ice monitor, a cylinder rotating freely around it's own axis, will probably never catch the events happening on the tip of a turbine blade. The difference in physical nature of the instrument compared to a turbine blade, is large. The tip speed of a rotor blade is significantly higher than that of the cylinder rotating around its own axis. All processes, sublimation, shedding, melting and acccreting, is faster on the turbine blades. The connection between icing and production loss is due to this very hard to find based on cylinder measurements.

Since the kriging model is based on empirical data, it resembles very well what is happening on the cylinder as production is changing, whereas the events on the turbine wing is not resembled very well. Improving the number and quality of observation data should improve the model significantly.

As predicting of ice is giving promising results by the use of weather prediction models. The empirical model calculating production loss should be able to predict the power output with input from the ice simulations. This can work well for the season as a whole. In short time intervals, however, the empirical data based model need to be improved.

Weather prediction models are found to often underestimate ice load. By investigating different output scenarios for specific wind speeds and ice loads, it is suggested that this is used in the weather prediction models to tune the estimated ice load to the correct level.

6.1 Further research

If a model should be developed based on empirical data, many improvements can be done.

- First of all, ice measurements need to improve. Mismatch between ice load on the cylinder and turbine wing is a large problem.
- Developing an adaptive model which can update itself as more measurements are collected should be investigated.
- Using icing rates to verify when an icing event starts, and for how long it lasts should be included. Then a factor could be added to "'speed up"' the model during accretion.
- Temperature measurements can be used with the same approach to include melting and shedding.

Losses due to icing are still thought to be underestimated. One suggestion to get a more accurate loss estimate, is to investigate alarm codes and include them correctly so that ice triggered alarms are calculated within the loss.

Bibliography

[Babinsky, 2003] Babinsky, H. (2003). How do wings work? *Physics Education*, 38:497–503.

[Barber et al., 2009] Barber, S., Wang, Y., Chokani, N., and Abhari, R. S. (2009). The effect of ice shapes on wind turbine performance. In *13th Int. Workshop on Atmospheric Icing*, Andermatt, Switzerland.

[Battisti et al., 2005] Battisti, L., Fedrizzi, R., Dell'Anna, S., and Rialti, M. (2005). Ice risk assessment for wind turbine rotors equipped with de-icing systems. In *BOREAS VII*, page 11, Saariselkä, Findland (2005). FMI.

[Boyle, 2004] Boyle, G. (2004). *Renewable Energy*. Oxford University Press.

[Bragg et al., 2007] Bragg, M., Broeren, A., Addy, H., Potapczuk, M., Guffond, D., and Montreuil, E. (2007). Airfoil ice-accretion aerodynamics simulation. Technical report, National Aeronautics and Space Administration.

[Broeren et al., 2006] Broeren, A. P., Bragg, M. B., and Addy, H. E. (2006). Flow-field measurements about an airfoil with leading-edge ice shapes. *J. Aircraft*, 43:1226–1234.

[Cressie, 1990] Cressie, N. (1990). The origins of kriging. *Mathematical Geology*, 22(2):239.

[Drage, 2005] Drage, M. A. (2005). *Atmospheric icing and meteorological variable Full scale experiment and testing of models*. PhD thesis, University of Bergen and Univercity center in svalbard.

[Efron, 1982] Efron, B. (1982). *The Jackknife, the Bootstrap and Other Resampling Plans*. Society of Industrial and Applied Mathematics, Philadelphia, PA.

[Fikke, 1980] Fikke, S. M. (1980). Ising og vind på luftledninger og tårn. *Været*, 4.

[Ghosh et al., 1984] Ghosh, M., Parr, W. C., Singh, K., and Babu, G. J. (1984). A note on bootstrapping the sample median. *The Annal of Statistics*, 12:1130–1135.

[Harstveit, 2002] Harstveit, K. (2002). Using routine meteorological data from airfields to produce a map of ice risk zones in norway. In *10th Int. Workshop on Atmos. Icing of Structures*, Brno, Czech Republic.

[Harstveit, 2009] Harstveit, K. (2009). Using metar-data to calculate in-cloud icing on a mountain site near by the airport. In *13th Int. Workshop on Atmospheric Icing*, Andermatt, Switzerland.

[Harstveit et al., 2009] Harstveit, K., Øyvind Byrkjedal, and Berge, E. (2009). Validation of regional in-cloud icing maps in Norway. In *13th Int. Workshop on Atmospheric Icing*, Andermatt, Switzerland.

[Homola et al., 2006] Homola, M. C., Nicklasson, P. J., and Sundsbø, P. A. (2006). Ice sensors for wind turbines. *Cold Regions Science and Technology*, 46(2):125 – 131.

[Homola et al., 2009] Homola, M. C., Ronsten, G., and Nicklasson, P. J. (2009). Energy production losses due to iced blades and instruments at Nygårdsfjell, Sveg and Aapua. In *13th International workshop on Atmospheric Icing*.

[Huang, 1991] Huang, J. C. (1991). Estimating the variance of the sample median, discrete case. *Statistics and Probability Letters*, 11:291–298.

[ISO12494, 2001] ISO12494 (2001). Iso standard atmospheric icing of structures. Technical report, International Organization of Standardisation.

[Jasinski et al., 1998] Jasinski, W. J., Noe, S. C., Selig, M. S., and Bragg, M. B. (1998). Wind turbine performance under icing conditions. *Journal of Solar Energy Engineering*, 120(1):6.

[Laakso et al., 2009] Laakso, T., Tallhug, L., Ronsten, G., Cattin, R., Baring-Gould, I., Lacroix, A., Peltola, E., Wallenius, T., and Durstewitz, M. (2009). Wind energy in cold climate iea task 19 outlook 2010. In *13th Int. Workshop on Atmospheric Icing*, Andermatt, Switzerland.

[Langmuir and Blodgett, 1960] Langmuir, I. and Blodgett, K. B. (1960). *The Collected Works of Irving Langmuir*, chapter A mathematical investigation of water droplet trajectories, page 335. Elmsford, N.Y.

[Makkonen, 1984] Makkonen, L. (1984). Modeling of ice accretion on wires. *Climate and applied Meteorology*, 23:929–939.

[Makkonen, 1987] Makkonen, L. (1987). Experiments on the cloud droplet efficiency of cylinders. *Climate and applied Meteorology*, 26:1406–1411.

[Makkonen, 1996] Makkonen, L. (1996). Modeling power line icing in freezing precipitation. In *7th Int. Workshop on Atmospheric Icing*, pages 195–200.

[Makkonen, 2000] Makkonen, L. (2000). Models for the growth of rime, glaze, icicles and wet snow on structures. *Phil. Trans. R. Soc. Lond.*, 358:2913–2939.

[Makkonen et al., 2001] Makkonen, L., Lakso, T., Marjaniemi, M., and Finstad, K. J. (2001). Modeling and prevention of ice accretion on wind turbines. *Wind engineering*, 25:3–21.

[Manwell et al., 2002] Manwell, J., McGowanand, J., and Rogers, A. (2002). *Wind Energy explained: Theory, Design and Application*, chapter 3, page 84. John Wiley & Sons, Ltd, Chichester, UK.

[Michalakes et al., 2001] Michalakes, J., Chen, S., , Dudhia, J., Hart, L., Klemp, J., Middlecoff, J., and Skamarock, W. (2001). Development of next generation regional weather research and forecast model. In *Ninth ECMWF workshop on the use of high performance computing in meteorology 2001*, pages 269–27, Singapore. world scientific.

[NSIDC, 2008] NSIDC (2008). Icing definition. url http://nsidc.org/arcticmet/glossary/icing.html.

[Nygaard, 2009] Nygaard, B. E. (2009). Evaluation of icing simulations for the "cost727" icing test sites in europe. In *13th Int. Workshop on Atmospheric Icing*, Andermatt, Switzerland.

[Parent and Ilinca, 2011] Parent, O. and Ilinca, A. (2011). Anti-icing and de-icing techniques for wind turbines: Critical review. *Cold Regions Science and Technology*, 65(1):88 – 96.

[Salby, 1996] Salby, M. L. (1996). *Fundamentals of Atmospheric Physics*. Academic Press.

[Seifert and Richert, 1998] Seifert, H. and Richert, F. (1998). A recipe to estimate aerodynamics and iceloads on iced rotor blades. In *BOREAS IV*, Hetta, Finland. Enontekiö.

[Siral, 2005] Siral (2005). Aapua vindpark. http://www.siral.se/2010/06/aapua-vindpark/.

[Stark and Woods, 2002] Stark, H. and Woods, J. W. (2002). *Probability and Random Processes with applications to Signal Processing*. Tom Robbins, 3rd edition.

[Stein, 1999] Stein, M. L. (1999). *Interpolation of spatial data: some theory for Kriging*. Springer, New York.

[Sundin and Makkonen, 1997] Sundin and Makkonen (1997). Ice loads on a lattice tower estimated by weather station data. *Journal of applied meteorology*, 37:523–529.

[Tallhaug, 2003] Tallhaug, L. (2003). Calculation of potential ice risk in norway. In *BOREAS VI*, page 8, Pyhätunturi, Finlad. FMI.

[Tammelin et al., 1998] Tammelin, B., Cavaliere, M., Kimura, S., Morganand, C., and Peltomaa, A. (1998). Ice free anemometers. In *Boreas IV*, page 125, Hetta, Finland. FMI.

[Tammelin and Seifert, 2001] Tammelin, B. and Seifert, H. (2001). Large wind turbines go into cold climate regions. In *EWEC 2001*. Copenhagen.

[Thompson et al., 2008] Thompson, G., Field, P. R., Rasmussen, R. M., and Hall, W. D. (2008). Explicit forecasts of winter precipitation using an improved bulk microphysics scheme. part ii: Implementation of a new snow parameterization. *Monthly Weather Review*, 136(12):5095–5115.

[Thompson et al., 2009] Thompson, G., Nygaard, B. E., Makkonen, L., and dierer, S. (2009). Using the weather research and forecasting (wrf) model to predict ground/structural icing. In *13th international workshop on atmospheric icing on structures*, Andermatt, Switzerland.

[Vestas, 2008] Vestas (2008). General specification V82 1.65 MW 1 speed. Technical report, Vestas Wind System AS.

[Virk et al., 2010] Virk, M. S., Homola, M. C., and Nicklasson, P. J. (2010). Effect of rime ice accretion on aerodynamic characteristics of wind turbine blade profiles. *Wind Engineering*, 34(2):207–218.

[Øyvind Byrkjedal, 2009] Øyvind Byrkjedal (2009). Estimating wind power production loss due to icing. In *13th Int. Workshop on Atmospheric Icing*, Andermatt, Switzerland.

[Øyvind Byrkjedal and Berge, 2009] Øyvind Byrkjedal and Berge, E. (2009). Meso-scale models shows promising results in predicting icing. In *EWEC 2009*, Marseille, France.